Russian Chemical Reviews **76** (11) 989 – 1011 (2007) © 2007 Russian Academy of Sciences and Turpion Ltd

DOI 10.1070/RC2007v076n11ABEH003720

Electronic mechanisms of molecular oxygen activation

B F Minaev

Contents

I.	Introduction	989
II.	Mechanisms of triplet – singlet transitions in the oxygen molecule	990
III.	Influence of collisions of oxygen molecule on intensities of forbidden transitions	994
IV.	Quenching of the $O_2(a^1\Delta g)$ molecule	1003
V.	Biochemical activation of the molecular oxygen	1005
VI.	Conclusion	1009

Abstract. Theoretical views on the mechanisms of overcoming spin prohibitions in photoprocesses and in enzymatic activation of the O_2 molecule are considered. The electronic structures of various quantum states of this molecule and collision complexes of oxygen with other molecules are given. The patterns of biochemical activation of O_2 through T – S transitions in enzymatic complexes are proposed. It is noted that the enhancement mechanisms for specific exchange interactions in enzymatic complexes have common features with mechanisms of physical photoactivation of oxygen. The bibliography includes 164 references.

I. Introduction

Specific physicochemical properties of the diatomic oxygen molecule are due to incompleteness of the outer π_g-electron shell.[1–9] Oxygen is paramagnetic[4] and can both quench and sensitise luminescence of organic compounds,[1,2] acts as a catalyst of some chemical transformations[6] and as an oxidant in many processes, in particular, breath, combustion and putrefaction, which occur at different rates and by different mechanisms.[5–7] Molecular oxygen is basic to life on Earth.[6] Indeed, it protects living organisms from hard solar radiation, absorbs the most part of UV radiation in upper atmosphere, generates the ozone layer that absorbs softer UV radiation in the stratosphere and, finally, provides the aerobic life with the energy of breath. However, since Lavoisier, who discovered the ability of the oxygen molecule to maintain breath and combustion, there is no clear understanding of the mechanisms of enzymatic activation of O_2, their relation to the electronic structure and spin of the molecule, to the fine structure of spin multiplet states of oxygen and to other physical (optical and magnetic) properties of this molecule.[3–21]

The present review is concerned with many aspects of photophysical and biochemical activation of O_2 associated with overcoming spin prohibitions. Photochemistry of singlet oxygen is only briefly outlined, because it was considered in recent reviews.[17–21]

Almost all reactions of oxygen molecule with chemically stable diamagnetic compounds are exothermic and require specific activation.[5–8] Combustion requires initial high-temperature activation of O_2 in the form of ignition (generation of primary radicals),[8] breath requires biochemical enzymatic activation;[5] in the case of autooxidation the activation is inefficient and slow.[6] Exothermicity of the oxidation reactions of organic substances is usually explained by high electronegativity of oxygen and by additional stabilisation of C – O and O – H bonds due to their higher polarity[6] compared to C – C and C – H bonds. It is believed[5,6] that, owing to high strength of the O – O bond in the O_2 molecule, the activation energies for reactions involving oxygen are too high for them to proceed at sufficiently high rates under normal conditions. However, the chemical inertness of the oxygen molecule is not due only to high bond energy, but also to spin restrictions.[3–5,12]

Clearly, aerobic life has appeared and exists due to specific kinetic prohibitions to reactions of paramagnetic oxygen with diamagnetic organic substances.[3,12] The main source of slowing down of the O_2 reactions is the spin prohibition, namely, the reactants have two unpaired spins (from O_2 molecule; electrons in substrate are paired), while in diamagnetic oxidation products all spins are always paired. The overcoming of this prohibition by introducing (generating) radicals to react with oxygen (burn) is inadmissible to living matter. Enzymes of a living cell find another way to overcome the spin prohibition to reactions of oxygen 'insertion' into diamagnetic organic substances. Therefore, establishment of the mechanisms of enzymatic bio-activation of oxygen requires investigations of spin effects.[3,12]

Nearly three decades ago the author of this review first explained intensity borrowing mechanism of magnetic dipole transitions[22–24] responsible for the known atmospheric absorption bands of oxygen.[11] Calculations of the structure of collision complexes of O_2 with diamagnetic substances[25–28] and their chemical reactions with account of spin – orbit coupling[29–33] underlie the theory that made it possible to find the ways of overcoming spin prohibitions in the case of weak intermolecular interactions and in the course of chemical reactions.[12,29,34–38] Recently, this theory has found numerous supports.[1,3,35–37,39–43]

B F Minaev Bogdan Khmelnitsky National University in Cherkassy, bul. Shevchenko 81, 18031 Cherkassy, Ukraine. Fax (38-0472) 35 44 63, tel. (38-0472) 37 65 76, e-mail: bfmin@rambler.ru

Received 16 April 2007
Uspekhi Khimii **76** (11) 1059 – 1083 (2007); translated by A M Raevskiy

This review conciders the electronic mechanisms of overcoming spin prohibitions to the reactions of O_2 and oxygen complexes with other molecules including solvent molecules and active sites of enzymes. Processes leading to acceleration of radiative and non-radiative triplet – singlet (T – S) transitions in O_2 molecule induced by collisions in the gas phase and in solution including sensitisation of singlet oxygen are generally termed 'photophysical activation'. We will also consider mechanisms of singlet oxygen luminescence and quenching, although these processes are in essence deactivation. The possibility of removal of spin prohibition in photophysical processes is treated as the first step towards understanding of biochemical enzymatic reactions of oxygen.[3, 24–37] In the review we also analyse the physical (mainly spectral) and chemical properties of O_2 molecule and the properties of other active forms of oxygen in relation to photoshemistry of atmosphere, combustion, catalysis and bio-oxidation.

II. Mechanisms of triplet – singlet transitions in the oxygen molecule

1. Energy characteristics of pure spin states of the oxygen molecule

Let us consider the ground- and excited-state electronic structure of O_2 molecule and factors determining the probability of T – S-transitions in free the oxygen molecule.

Back in 1848, Faraday weighed various gases with a magnetic balance and established that, unlike many other elements, molecular oxygen is paramagnetic.[6] An explanation for this amazing fact was reported much later.[4] Mulliken explained paramagnetism of molecular oxygen by considering the ground-state configuration in which the highest occupied molecular orbital (MO) is a doubly degenerate π_g orbital occupied by two electrons.[4] In this case the inclusion of a 'molecular' analogue of Hund's rule leads to parallel electron spin orientations in the lowest-energy state. Thus, atmospheric oxygen contains O_2 molecules in the triplet ground state corresponding to the following electronic configuration [4, 22]

$$\Psi = (1\sigma_g)^2(1\sigma_u)^2(2\sigma_g)^2(2\sigma_u)^2(3\sigma_g)^2(1\pi_u)^4(1\pi_g)^2. \quad (1)$$

There are four possible quantum states of the molecule with particular values of the spin (S) and orbital (L_z) angular momenta [4] depending on arrangement of two outer electrons in two degenerate $1\pi_g$-MOs. Using complex wave functions of MO in the form [15]

$$\pi_g^{\pm} = \psi(r,\theta)e^{\pm i\phi}, \quad (1a)$$

where θ is the angle between the z axis and the radius vector $\boldsymbol{r}$, ϕ is the angle of rotation of the radius vector $\boldsymbol{r}$ about the molecular axis z, these states can be represented by the following qualitative models:

$$\begin{array}{cccc} [\uparrow][\uparrow] & [\uparrow\downarrow][\ ] & [\ ][\uparrow\downarrow] & [\uparrow][\downarrow] \\ |^3\Sigma_g^-\rangle & |^1\Delta_g\rangle & |^1\Delta_g\rangle & |^1\Sigma_g^+\rangle \end{array} \quad (2)$$

Here the quantum cells [ ][ ] denote degenerate $\pi_g^{\pm}$-orbitals. The respective complex determinant wave functions for the open shells of the states (2) have the form [4, 10]

$$^3\Sigma_g^- = \frac{1}{\sqrt{2}}\left(|\pi^+\bar{\pi}^-| - |\pi - \bar{\pi}^+|\right), \quad (2a)$$

$$^1\Delta_g = |\pi^+\bar{\pi}^+|,$$

$$^1\Delta_g = |\pi^-\bar{\pi}^-|,$$

$$^1\Sigma_g^+ = \frac{1}{\sqrt{2}}\left(|\pi^+\bar{\pi}^-| + |\pi^-\bar{\pi}^+|\right).$$

Here | | is the conventional notation of the determinant wave functions,[10] $\pi^{\pm}$ denotes the α-spin MO (spin-up MO) and $\bar{\pi}^{\pm}$ denotes the β-spin $\pi_g^{\pm}$-MO (spin-down MO). The functions (2a) are eigenfunctions of the operator of the orbital angular momentum projection (L_z) with the quantum number $\Lambda = 0$ (for the states $\Sigma_g^{\pm}$) and 2 (for the states $^1\Delta_g$)[4, 10–16] in $\hbar = h/2\pi$ units (h is the Planck constant). With allowance for exchange interaction between two π_g-electrons, the triplet state $^3\Sigma_g^-$ has the lowest energy, thus being the ground state; the next is the doubly degenerate singlet state $^1\Delta_g$, while the singlet state $^1\Sigma_g^+$ has the highest energy.[4, 9]

The total spin quantum number (S) in the expression for the eigenfunctions of the operator $\boldsymbol{S}^2$

$$\boldsymbol{S}^2\Psi = S(S+1)\hbar^2\Psi \quad (3)$$

is equal to zero for singlets and to unity, for triplets.[15] Functions (2a) obey relation (3), their multiplicity (left superscript) is $2S + 1$. Qualitative description of energy characteristics of O_2 can be obtained [22] using simple semiempirical quantum chemical methods, *e.g.*, INDO.[15] The inclusion of configuration interaction (CI) with the basis set (2) leads to the same splitting between the three states $|^3\Sigma_g^-\rangle$, $|^1\Delta_g\rangle$, $|^1S_g^+\rangle$, equal to the atomic exchange integral:[13] $(p_x p_y|p_x p_y) = 0.8$ eV. The energies of the singlet states $|^1\Delta_g\rangle$ and $|^1\Sigma_g^+\rangle$ calculated relative to the triplet ground-state energy are 0.8 and 1.6 eV, respectively,[22] which agrees with experimental data (0.98 and 1.63 eV, respectively).[9] The agreement is improved by inclusion of configuration interaction and the $\ldots(1\pi_u)^2(1\pi_g)^4$ configuration, however the pattern of the wave functions remains essentially the same.[12] The following is quite important. Computational quantum chemistry methods usually employ real wave functions for the atomic basis set p_x, p_y and p_z.[15] The singlet states are described by the following combinations of the wave functions:[10, 22]

$$|^1\Delta_g\rangle = {}^1\Phi_1 = \frac{1}{\sqrt{2}}\left(|\pi_x\bar{\pi}_x| - |\pi_y\bar{\pi}_y|\right), \quad (4)$$

$$|^1\Delta_g\rangle = {}^1\Phi_2 = \frac{1}{\sqrt{2}}\left(|\pi_x\bar{\pi}_y| + |\pi_y\bar{\pi}_x|\right), \quad (4a)$$

$$|^1\Sigma_g^+\rangle = {}^1\Phi_3 = \frac{1}{\sqrt{2}}\left(|\pi_x\bar{\pi}_x| + |\pi_y\bar{\pi}_y|\right), \quad (5)$$

$$|^3\Sigma_g^-\rangle = {}^3\Phi_0 = \frac{1}{\sqrt{2}}\left(|\pi_x\bar{\pi}_y| - |\pi_y\bar{\pi}_x|\right),$$

where π_x denotes the spin-up (α-spin) $1\pi_{gx}$-MO and $\bar{\pi}_x$ denotes the spin-down (β-spin) $1\pi_{gx}$-MO. The real π_g-MO functions in the INDO approximation have a simple form [22]

$$\pi_x = \frac{1}{\sqrt{2}}\left(p_x^A - p_x^B\right), \quad (6)$$

$$\pi_y = \frac{1}{\sqrt{2}}\left(p_y^A - p_y^B\right),$$

where p_x^A denotes the real 2p-AO of the atom A, oriented along the x axis and the symbols 'A' and 'B' denote the two oxygen atoms. Electrons of the closed shell in Eqns (4) and (5) are omitted because they do not affect the matrix elements of the one-electron operators [dipole moment, angular momentum, spin – orbit coupling (SOC)]. For the triplet ground state $|^3\Sigma_g^-\rangle$, the form of the determinant functions (2) and (5) remains unchanged, whereas the functions for the singlet states (2) in

the real basis set (6) have another form. This feature should be taken into account [12] in calculations of (i) collision complexes of oxygen molecule with other molecules and (ii) chemical reactions involving this molecule.

The complex functions (1a) and (2) are only convenient in the case of isolated O_2 molecule. By expanding determinants in relationships (5), one can separate the orbital and spin contributions; then the singlet and triplet Σ-states have the form

$$|^1\Sigma_g^+\rangle = {}^1\Phi_3 =$$

$$= \frac{1}{\sqrt{2}}\left[\pi_x(1)\pi_x(2) + \pi_y(2)\pi_y(1)\right]\frac{1}{\sqrt{2}}\left[\alpha(1)\beta(2) - \alpha(2)\beta(1)\right], \quad (5a)$$

$$|^3\Sigma_g^-\rangle = {}^3\Phi_0 =$$

$$= \frac{1}{\sqrt{2}}\left[\pi_x(1)\pi_y(2) - \pi_x(2)\pi_y(1)\right]\frac{1}{\sqrt{2}}\left[\alpha(1)\beta(2) + \alpha(2)\beta(1)\right]. \quad (5b)$$

The '+' and '−' signs at the term 'Σ' denote mirror symmetry relative to any plane containing the molecular axis, *e.g.*, the *yz* plane. Reflection in this plane causes the π_x-MO to change its sign while the sign of the π_y-MO remains unchanged. Because of this, both components in the orbital part of the wave function (5b) change their signs; *i.e.*, this function is antisymmetrical with respect to reflection in plane, while the wave function (5a) is symmetrical. The same conclusions can be drawn by considering the *xz* plane. As to the complex functions (1a) and (2a), these conclusions are valid for any plane containing the molecular axis,[15] because reflection in plane causes replacement of ϕ by $-\phi$ and, hence, replacement of π^+ by π^- in relation (1a).

Thus, for planar collision complexes of O_2 the real wave functions (5) characterise the key symmetry properties of the low-lying electronic states of this molecule. Selection rules for functions (1) and (2) are also valid for functions (4)−(6). Collision complexes have no inversion point. This formally breaks quantisation of the projection of the orbital angular momentum and in polyatomic molecules the quantum number of the operator L_z is no longer a 'good quantum number'.[13] However, calculations [27–31] revealed only minor changes in the structure of the wave functions (4) and (5) and in the energies of corresponding states of collision complexes. Therefore, the collision complexes can be treated using the same notations of terms (4) and (5) as those of free O_2 molecule.

Specific behaviour of O_2 molecule in animated nature is mainly due to the presence of low-energy excited singlet states and the intrinsic magnetic moment (spin) in the ground state (paramagnetism of O_2).[12,27] Figure 1 presents the potential curves for certain states of the O_2 molecule, obtained from multiconfiguration self-consistent field (MC SCF) calculations with subsequent inclusion of configuration interaction.[30,40] High-energy excited states $^{3,1}\Sigma_u^-$ and $^3\Delta_u$, $^3\Sigma_u^+$ responsible for UV emission of oxygen (Herzberg bands) are of great interest for atmosphere photochemistry and gas discharge spectroscopy.[9,39–42] When discussing the photochemistry of singlet oxygen ($^1\Delta_g$), these states are usually left out of consideration, although from the standpoint of spin catalysis theory [32–34] they should also be taken into account. The triplet state $B^3\Sigma_u^-$ gives an allowed electric dipole transition $B^3\Sigma_u^- \leftarrow X^3\Sigma_g^-$ (Ref. 9) responsible for the Schumann–Runge absorption band. Due to this intense absorption in upper atmosphere, hard solar UV radiation (135–190 nm) does not arrive to the Earth's surface. Since minima on the potential curves for the *B*- and *X*-states are strongly shifted relative to one another

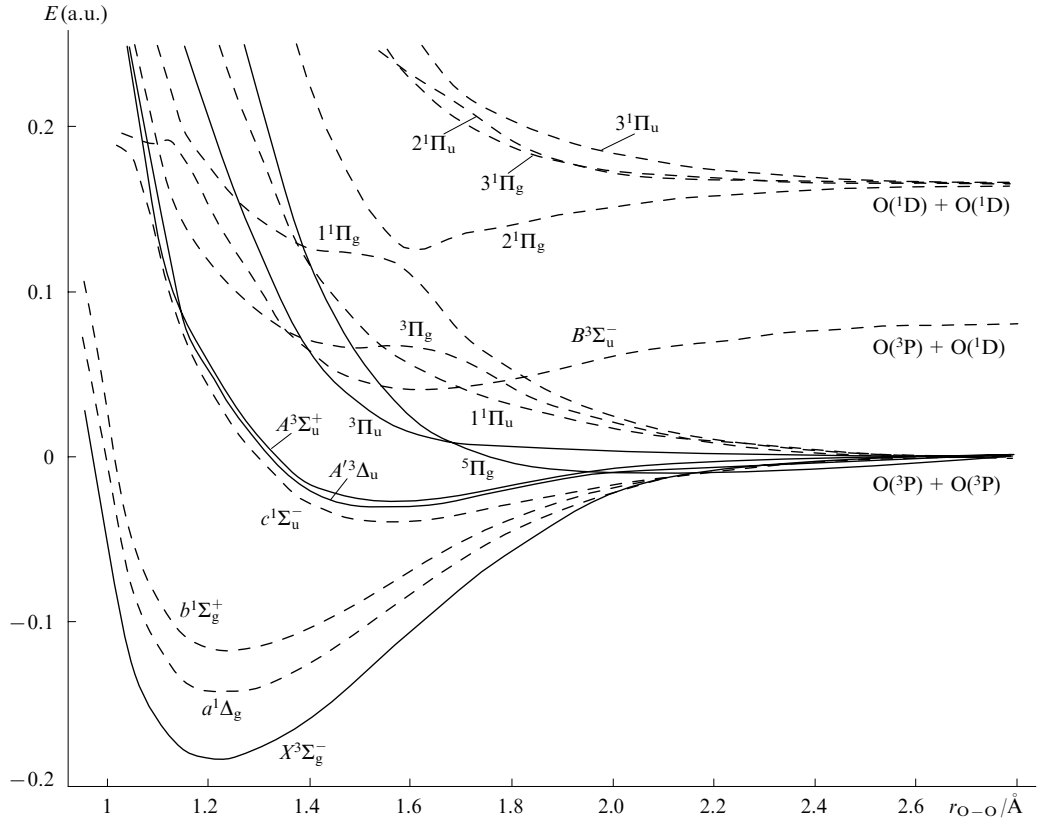


Figure 1. Potential curves for certain quantum states of O_2 molecule obtained from *ab initio* calculations.[30,31]
Literal notations of terms used here and in Fig. 2 are common to molecular spectroscopy. Main multiplet states: singlet (*a*, *b*, *c*) and triplet (*A*, *B*).

(see Fig. 1), the vertical transition $B^3\Sigma_u^-/X^3\Sigma_g^-$ leads to dissociation of O_2 molecule. In addition, pre-dissociation of bound vibrational states of the upper term is also possible due to crossing with the potential curves of the Π_u-states.[9]

Various glow phenomena in the night sky including auroral ones are due to decomposition of oxygen molecule to atoms and subsequent recombination of oxygen atoms with the formation of excited O_2 molecules.[9] In this review, we will leave these interesting phenomena out of consideration. Mention may only be made that theory of forbidden transitions from the $c^1\Sigma_u^-$, $A'^3\Delta_u$ and $A^3\Sigma_u^+$ excited states provides a great body of valuable information on the SOC mechanisms[12] that are important for understanding of the enzymatic activation of oxygen. In addition to the Herzberg bands, red atmospheric bands of oxygen [transition $b^1\Sigma_g^+ \rightarrow X^3\Sigma_g-$ (762 nm)] and IR radiation (transition $a^1\Delta_g \rightarrow X^3\Sigma_g^-$ at 1270 nm) were detected.[9] Long optical path in the atmosphere also allows these bands to be clearly defined in absorption (the red band represents a combination of certain Fraunhofer lines) in spite of the forbiddenness and low probability of these transitions.

Until recently, the singlet state of oxygen was of interest only for researchers working in atmosphere optics.[10,11] In 1976, Krasnovsky [14] first detected luminescence of singlet oxygen ($a^1\Delta_g$) in solution. At present, singlet oxygen is used in technics,[1,17,18] chemistry [17–21] and medicine.[1,19,43] Singlet oxygen molecule $O_2(a^1\Delta_g)$ is known as oxidant in chemical and biological processes, because the spin prohibition is removed and the species is more reactive than the triplet atmospheric oxygen molecule $O_2(X^3\Sigma_g^-)$.[1–7,19–21] Taking into account four quantum states (2) of oxygen molecule is required for not only understanding of oxygen photochemistry, but also development of theory of the dark chemical reactions,[12,29,32] in particular, for studies of enzymatic oxidation proceeses.[37]

2. Intensities of singlet – triplet transitions in optical spectra of the oxygen molecule

To understand the mechanism of removal of spin prohibitions in chemical reactions involving oxygen, one should consider a theory of intensity of singlet – triplet transitions in isolated O_2 molecule and the effect of solvent on these transitions.[22–96] Radiative transitions between all states (2) are strictly forbidden in the electric dipole approximation,[11,43] because all of them have the same parity (gerade symmetry relative to inversion point), whereas the selection rules require a change in parity upon transitions. For electric dipole transitions the projection of the orbital angular momentum on the molecular axis (Λ) should vary by $\Delta\Lambda = \pm 1, 0$. The $^1\Delta - ^1\Sigma^+$ transition is also forbidden due to the selection rule for the projection of the orbital angular momentum ($\Delta\Lambda = 2$). In free O_2 molecule, this transition is detected as a weak quadrupole transition because in the quadrupole approximation the prohibition for $\Delta\Lambda = 2$ is removed.[12,26] Singlet – triplet transitions between terms (2) are additionally forbidden by the spin selection rule, $\Delta S = 1$. Transition between states (5) is also forbidden by the $\Sigma^- - \Sigma^+$ rule, *i.e.*, we deal with the triple prohibition.

All the prohibitions mentioned above are strict.[49] The more long-wavelength singlet – triplet transition $^1\Delta_g - ^3\Sigma_g^-$ is additionally forbidden by the selection rule for the orbital angular momentum ($\Delta\Lambda = 2$) and thus characterised by triple prohibition [with respect to spin, parity (gerade – gerade) and orbital angular momentum, that is, $\Delta\Lambda = 2$] in the electric dipole approximation. A diagram of different quantum states (4), (5) and transitions between them for the collision complex of O_2 molecule and a dye is shown in Fig. 2. Both singlet – triplet transitions, $a - X$ and $b - X$, should be very weak due to the triple prohibition on emission in the dipole approximation.

The potential curves (see Fig. 1) for all the three states (X, a and b) are only slightly shifted relative to one another, the equilibrium internuclear distances (r) being respectively equal to 1.207, 1.216 and 1.227 Å (see Ref. 9). Therefore, only the 0 – 0 bands corresponding to electronic vibrational transitions between these states are intense in optical spectra.[9,42,46] The rate constant (k) for spontaneous emission $a \rightarrow X$ obtained by interpolation to zero oxygen pressure (no collisions; intermolecularly unperturbed O_2 molecule) was found to be record-low ($k_{a\rightarrow X} = 2.6 \times 10^{-4}$ s^{-1}).[17] The $b \rightarrow X$ transition is much more intense ($k_{b\rightarrow X} = 8.9 \times 10^{-2}$ s^{-1}). The radiative lifetimes [17] of the a and b states are 4600 and 12 s, respectively. The $a \rightarrow X$ and $b \rightarrow X$ transition intensities were first calculated in Ref. 22. In spite of semiempirical character of the wave functions used in the INDO method, the results of calculations [22] correctly describe the mechanisms of overcoming spin prohibitions, as was confirmed later by the results of *ab initio* calculations.[42,50,57] To understand the spin mechanisms of photo- and bio-activation of oxygen, we will consider the key points of the semiempirical theory.[22]

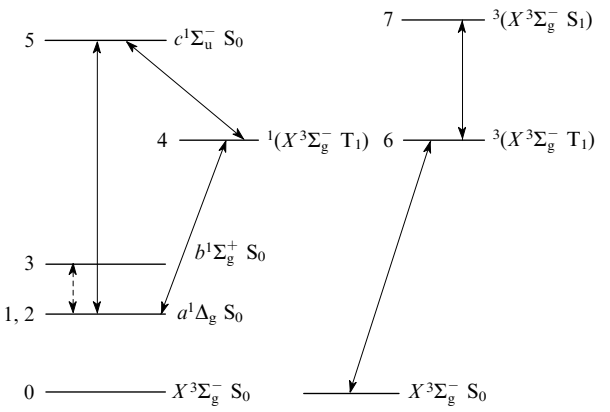


Figure 2. Scheme of quantum states in a collision complex of O_2 with a dye.

Symmetry analysis of the wave functions revealed the possibility of mixing of the singlet and triplet states (5) due to the SOC operator.[49] For simplicity, we will write this operator in the effective one-electron form [12,23]

$$H_{so} = \sum_A \zeta_A \sum_i \vec{l}_{i,A}\vec{s}_i = \sum_i \vec{B}_i\vec{s}_i = \quad (7)$$
$$= \sum_i (B_{i,x}s_{i,x} + B_{i,y}s_{i,y} + B_{i,z}s_{i,z}),$$

where ζ_A is the SOC constant for the atom A ($\zeta_O = 153$ cm^{-1}), $\vec{l}_{i,A}$ and $\vec{s}_i$ are respectively the operators of the orbital angular momentum and spin angular momentum of the ith electron.[12] The one-electron SOC operator (7) with inclusion of the constants ζ_A determined from atomic spectra gives quite reliable results suitable for explanation of numerous SOC effects in molecules.[12,13,49] The spin – orbit coupling between the singlet and triplet ($b^1\Sigma_g^+ - X^3\Sigma_{g,0}^-$) states [see relations (5)] is given by [22]

$$\langle {}^3\Sigma_g^- | H_{so} | {}^1\Sigma_g^+ \rangle = \langle {}^3\Phi_0 | H_{so}^Z | {}^1\Phi_3 \rangle = \quad (8)$$
$$= \langle \pi_x | B_z | \pi_y \rangle = -i\zeta_O = -153i \text{ cm}^{-1}.$$

Equation (5) was written for the triplet state with the zero projection of the total spin on the molecular axis (z axis).[22] In the text below this spin sublevel with the quantum number $M_S = 0$ will be designated by $|^3\Sigma_{g,0}^-\rangle$ (for the frame of reference associated with the O_2 molecule) and t_z (if the z axis of the frame of reference in the collision complexes of O_2 with organic reactant molecules matches the line of the O – O bond). The

other two spin sublevels of the triplet state with the quantum numbers $M_S = \pm 1$ in the oxygen molecule are degenerate; we will denote them $|^3\Sigma_{g,1}^-\rangle$. The separation between them and the $M_S = 0$ level equals the zero-field splitting (ZFS) energy,[9,22] which for the oxygen molecule is rather high (3.97 cm^{-1}; *cf.* a conventional value of 0.1 cm^{-1} for the triplet-excited states of aromatic molecules [13]). The ZFS is due to the dipole–dipole magnetic interaction between two unpaired spins.[49] In the case of O_2 molecule the SOC also contributes largely to the ZFS at the second-order level of perturbation theory.[48] Recently, correct *ab initio* calculations of the ZFS energy for oxygen molecule have been reported.[46] Among previous calculations presented in Refs 47–49, a number of errors are found, whereas semiempirical estimates [22,59] appeared to be more reliable.[13,46] Seemingly, the results of *ab initio* calculations [47] are in good agreement with the observed ZFS; however, this is a random coincidence. Indeed, the SOC contribution to ZFS is overestimated (doubled) owing to incorrect value of a factor. Correct calculation of magnetic perturbations in the ZFS is important for understanding of the mechanism of removal of spin prohibition for the singlet–triplet transitions in oxygen.

The matrix element of the operator of the SOC between the $\Sigma^- - \Sigma^+$ triplet and singlet states differs from zero only for the states (5) characterised by the quantum number $M_S = 0$. At the first-order level of perturbation theory, the wave functions of these states are mixed due to SOC [22]

$$\Psi_b = |b^1\Sigma_g^+\rangle + c|X^3\Sigma_{g,0}^-\rangle, \tag{9}$$

$$\Psi_{X,0} = |X,^3\Sigma_{g,0}^-\rangle - c^*|b^1\Sigma_g^+\rangle, \tag{10}$$

where the mixing coefficient

$$c = \frac{\langle X^3\Sigma_{g,0}^-|H_{so}|b^1\Sigma_g^+\rangle}{E(b^1\Sigma_g^+) - E(X^3\Sigma_{g,0}^-)} \tag{11}$$

is small (E is the energy of the corresponding state). With allowance for the semiempirical estimate of the SOC using Eqn (8) and energy difference [9] in the denominator of Eqn (11) (13 195 cm^{-1}), one gets [22] $c = -0.0116\,i$. The small value of the coefficient c provides an excellent substantiation of the applicability of perturbation theory and the wave functions (9) and (10) are characterised by rather high accuracy and correct normalisation. According to *ab initio* calculations,[42,50] the SOC matrix element [numerator in Eqn (11)] equals $-178\,i$ cm^{-1}, the absolute value of coefficient c being somewhat increased: $|c| = 0.0135$. This coefficient plays a key role in the theory of singlet–triplet transitions of oxygen molecule in the gas phase at low and high pressures and in O_2 solutions in organic compounds and biopolymers.[22–31]

Let us consider a magnetic dipole transition from the state (9) to the state $|^3\Sigma_{g,1}^-\rangle$ with the quantum number $M_S = \pm 1$. Unlike the spin sublevel $|^3\Sigma_{g,0}^-\rangle$, the $|^3\Sigma_{g,1}^-\rangle$ state is almost 'pure', *i.e.*, it contains minor contributions of singlet states. (Actually, it has a small contribution of the $^1\Pi_g$ state, but this is of no concern for the simplified treatment [22] of the $b-X$ transition.) The magnetic dipole moment operator

$$\boldsymbol{M} = \mu_B(\boldsymbol{L} + 2\boldsymbol{S}),$$

where μ_B is the Bohr magneton, contains the orbital ($\boldsymbol{L}$) and spin ($\boldsymbol{S}$) contributions. According to calculations,[22,42,50] the orbital contribution to the moment of the $b^1\Sigma_g^+ - X^3\Sigma_{g,1}^-$ transition is negligible. The major contribution to the $b-X$ transition intensity comes from the spin component [22] with the magnetic moment polarisation vector directed perpendicular to the molecular axis. Taking into account expression (9), one has [22]

$$\boldsymbol{M}_{b-X,1} = \mu_B\langle\Psi_b|2\boldsymbol{S}|\Psi_{X,1}\rangle = \tag{12}$$

$$= \mu_B\sqrt{2}c\langle X^3\Sigma_{g,0}^-|S_x \pm iS_y|X^3\Sigma_{g,1}^-\rangle = -2\mu_B c.$$

Thus, the $b^1\Sigma_g^+ - X^3\Sigma_{g,1}^-$ transition in the visible region (red atmospheric band of oxygen at 760 nm) in fact 'borrows' its intensity from the microwave transition between the spin sublevels $^3\Sigma_{g,0}^- - ^3\Sigma_{g,1}^-$ (magnetic dipole EPR transition induced by the spin operator). The calculated transition moment $\boldsymbol{M}_{b-X,1} = -0.027\,\mu_B$ is almost equal to the value obtained from intensity measurements.[9] This is a unique example in molecular spectroscopy; here the intensity of an optical electronic transition is determined by the EPR spin current intensity. This provides an explanation for a higher probability of the $b-X$ transition compared to that of the $a-X$ transition. In the latter case there is only a small orbital contribution to the magnetic dipole moment of the transition, due to the SOC-induced mixing of the a, X and $^{3,1}\Pi_g$ states.[22] Owing to large energy differences between these states

$$E(^1\Pi_g) - E_X = 78\,000\ cm^{-1},$$

$$E(^3\Pi_g) - E_a = 48\,000\ cm^{-1},$$

mixing of the singlets and triplets is negligible and the spin prohibition to the $a-X$ transition remains strict.

One should also consider the probability of the $b-a$ transition, which plays an important role in analysis of the solvent effect on the oxygen spectra. The $b-a$ transition of a free O_2 molecule is responsible for the appearance of a weak Noxon band, which is a quadrupole [26,89] with the maximum possible quadrupole moment.[26] However, the rate constant for spontaneous emission $b \to a$ obtained by interpolation to zero pressure is very small ($k_{b\to a} = 1.7\times10^{-3}\ s^{-1}$).[9] Theoretical studies [25–28] revealed that this transition should be dramatically enhanced upon collision of O_2 molecule with any diamagnetic molecule. Later on, this conclusion was confirmed experimentally for the gas,[39] solid [51,52] and liquid phases.[1,17,43,56]

With allowance for the SOC in the framework of perturbation theory one can explain the intensities of many UV bands of oxygen molecule.[30,31,59,65,67,91–96] In addition to calculations of well-known Herzberg bands,[9,30,49,65,67] a reliable explanation was obtained for the intensities of some new bands originated from recently detected new electronic transitions from the metastable state (9), namely, $b^1\Sigma_g^+ - B^3\Sigma_u^-$ and $b^1\Sigma_g^+ - c^1\Sigma_u^-$ (Refs 31, 91–95). The $b^1\Sigma_g^+ - B^3\Sigma_u^-$ transition proceeds by the mechanism of intensity 'stealing' from the Schumann–Runge band ($X-B$) due to the SOC (9); the coefficient c [see Eqn (11)] gives a correct order of magnitude [31,92] for the electric dipole moment of this transition. The $b^1\Sigma_g^+ - c^1\Sigma_u^-$ transition is also electric dipole in nature; removal of the $\Sigma^- - \Sigma^+$-type prohibition for the singlet–singlet transition is due to electronic-rotational coupling [95]

$$\left\langle \tilde{c}^1\Sigma_u^- \middle| \sum_i er_i \middle| \tilde{b}^1\Sigma_g^+ \right\rangle =$$

$$= \sum_n \frac{\langle n^1\Pi_g|BL_+|b^1\Sigma_g^+\rangle}{E(b^1\Sigma_g^+) - E(n^1\Pi_g)} \left\langle c^1\Sigma_u^- \middle| \sum_i er_i \middle| n^1\Pi_g \right\rangle +$$

$$+ \sum_k \frac{\langle k^1\Pi_u|BL_+|c^1\Sigma_u\rangle^*}{E(c^1\Sigma_u^-) - E(k^1\Pi_u)} \left\langle k^1\Pi_u \middle| \sum_i er_i \middle| b^1\Sigma_g^+ \right\rangle.$$

Here er_i is the dipole moment of the ith electron and B is the rotational constant.

Detection [94] and theoretical identification [95] of the $b^1\Sigma_g^+ - c^1\Sigma_u^-$ transition bands opens new prospects for atmosphere photochemistry studies. However, no $A^3\Sigma_u^+ - c^1\Sigma_u^-$ electronic transition in the IR region (2400 cm^{-1}) was detected so far, although the corresponding intensity stealing mechanism was developed two decades ago.[12] The magnetic dipole moment of this transition ($\boldsymbol{M}_{A-c} = 0.12\,\mu_B$) is about five times larger than that of the $b-X$ transition [see Eqn (12)]. The intensity stealing and the spin-prohibition removal mechanisms are very similar to those described by relations (9)–(12); however, this only concerns the $A^3\Sigma_u^+$ and $c^1\Sigma_u^-$ states. The SOC matrix element between these states is equal to the integral (8) while the energy difference in the denominator is very small (2400 cm^{-1}); this is the reason for high extent of intensity stealing from the transitions between spin sublevels of the $A^3\Sigma_u^+$ state (see Refs 12 and 91). The aforesaid is valid for a free O_2 molecule in a highly rarefied gas (upper atmosphere), when collisions can be ignored. Under normal pressure at Earth's surface, collisions with other molecules (O_2, N_2, water vapour) significantly affect the intensities of certain absorption bands of oxygen.[25–43, 51–56]

III. Influence of collisions of oxygen molecule on intensities of forbidden transitions

1. The Noxon transition

Let us consider simple models for collision complexes of O_2 with diamagnetic molecules.[1, 28, 39, 51, 58, 89, 97–109] Changes in the orbitals of the open π_g-shell of oxygen molecule upon its collision with the nitrogen molecule are shown in Fig. 3. For simplicity, we assume that the collision complex has a planar geometry and lies in the xz plane. All subsequent conclusions are also valid for arbitrary geometry of the complex. The moment of the Noxon transition $a^1\Delta_g - b^1\Sigma_g^+$ of the collision complex radically changes its nature, following the changes in the nature of orbitals of the open π_g-shell. In addition to the pure quadrupole component $\langle {}^1\Delta_g|Q|{}^1\Sigma_g^+\rangle$, which is the same for both terms (4) and (4a), the electric dipole component $\langle {}^1\Delta_g|D|{}^1\Sigma_g^+\rangle$ appears, which can differ for the two quasi-degenerate components of the singlet state a. The matrix elements of the dipole moment operator

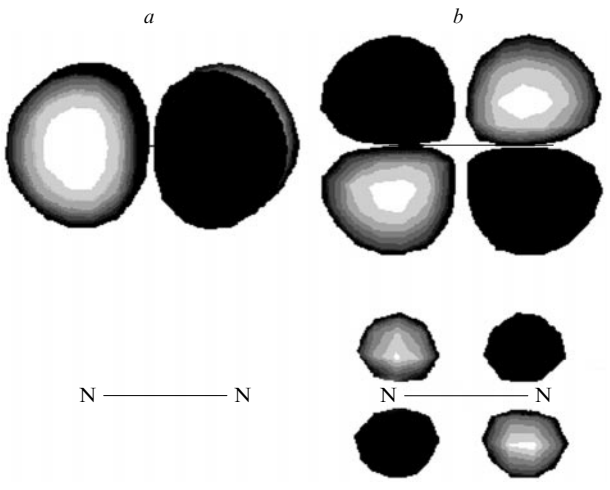


Figure 3. Molecular orbitals, $\pi_{g,y}$ (*a*) and $\pi_{g,x}$ (*b*), of O_2 in collision complex of oxygen and nitrogen molecules.
The z axis matches the N_2 molecular axis; the y axis is normal to the xz plane of the complex. White and dark background corresponds to the positive and negative signs of the wave functions.

$$D = e\sum_i r_i = \sum_i d_i$$

for the singlet–singlet ($a^1\Delta_g - b^1\Sigma_g^+$) transition [see Eqns (4) and (5)] are equal to the dipole moment difference between two π_g-MOs (see Ref. 28)

$$\langle {}^1\Phi_1|D|{}^1\Phi_3\rangle = \langle \pi_x|d|\pi_x\rangle - \langle \pi_y|d|\pi_y\rangle. \quad (13)$$

For the second component of the $a^1\Delta_g$ state [see Eqn. (4a)] the dipole moment of the $a-b$ transition is

$$\langle {}^1\Phi_2|D|{}^1\Phi_3\rangle = \langle \pi_y|d|\pi_x\rangle + \langle \pi_x|d|\pi_y\rangle. \quad (14)$$

For the planar collision complex $O_2 + N_2$ (see Fig. 3), the dipole moment difference between two oxygen π_g-MOs differs from zero. Spin-restricted Hartree–Fock [87] calculations of the triplet ground state of the complex $O_2 + N_2$ (see Fig. 2) revealed significant deformation of the $\pi_{g,x}$-orbital of the O_2 molecule due to mixing with orbitals of the nitrogen molecule (see Fig. 3 *b*), whereas the $\pi_{g,x}$-MO remains almost unchanged (see Fig. 3 *a*).[12, 27] The overlap of the π_x-orbitals of the two molecules (σ-type overlap, see Fig. 3 *b*) is much larger than that of the π_y orbitals (π-type overlap).

The structures of the states (4) and (5) determined with allowance for configuration interaction remain almost unchanged.[12] The dipole moment of the $\pi_{g,x}$-orbital differs from zero, because it includes quite large contributions of nitrogen atoms; despite small coefficients in the LCAO expansions for these atoms, the dipole moment $\langle \pi_x|d|\pi_x\rangle$ of the $\pi_{g,x}$-orbital is of great importance because of the long intermolecular distance (R = 2.8 Å). The moment of the transition (13) reaches a value of 0.1 D, the transition intensity being four orders of magnitude higher than the intensity of the pure quadrupole transition $a^1\Delta_g - b^1\Sigma_g^+$ of free O_2 molecule.[12] This example (see Fig. 3) provides the simplest illustration of the Noxon band (transition $a^1\Delta_g - b^1\Sigma_g^+$) enhancement mechanism in the collision complex due to the appearance of the electric dipole moment of the transition. At arbitrary collision geometry, both terms on the right side of Eqns (13) and (14) differ from zero, but the total intensity of the Noxon band mainly depends on R. The off-diagonal matrix elements of the one-electron operator of the dipole moment between the π_g-orbitals of the open shell of oxygen [see Eqn (14)] depend on the extent of deviation of the collision complex geometry from planar one (see Fig. 3). This is also characteristic of most molecules having more complex structures compared to N_2. For instance, an oxygen–butadiene collision complex cannot have planes among symmetry elements (only the most probable non-planar π-complex is considered here); in this case the integrals (13) and (14) are commensurable.[87]

The extent of the Noxon band enhancement depends on the polarisability (α_{cp}) of the partner in collision.[1, 17, 87, 98] This was revealed by the first MINDO/3 calculations with inclusion of configuration interaction for singly and doubly excited configurations.[28] Qualitative correlation between the Noxon band enhancement and an increase in the ionisation potential of the partner in collision (molecular polarisability increases as the ionisation potential decreases) was pointed out.[13] The dipole moment $\langle \pi_x|d|\pi_x\rangle$ of the oxygen $\pi_{g,x}$-orbital in the complex with nitrogen (see Fig. 3) depends on the contribution of the vacant nitrogen π_g-MO, which is in turn determined by the polarisability of this molecule.[87, 98] Enhancement of the Noxon band with an increase in the collision-partner polarisability [28, 87, 98–101] was even better demonstrated in analysis of the results of CI calculations [12, 97, 98] in the oxygen complexes with helium and hydrogen.

2. Effect of collisions on intensities of singlet – triplet transitions of oxygen in the visible and near IR optical spectra

Singlet molecular oxygen in the $a^1\Delta_g$ state is produced by photosensitisation of dye solutions.[1,28] This species plays a key role in some photochemical and photobiological processes.[53–56] Such diseases as skin cancer and cataract as well as ageing are associated with reactions involving $O_2(a^1\Delta_g)$.[17–21] Recently, this form of oxygen has been used in organic synthesis, in bleaching, in medicine for treatment of malignant tissues (photodynamic therapy),[1,18,19] as an air pressure gauge in aerodynamics,[17,105] as fixing agent in high-spatial and high-temporal resolution microscopes [56,82,83] and as a microscopic luminescing detector.[1,17]

Wide use of singlet oxygen is due to unique properties of the singlet – triplet transition $a^1\Delta_g \rightarrow X^3\Sigma_g^-$. As mentioned above, this transition of free O_2 molecule (at zero pressure) is characterised by very low emission (rate constant for spontaneous emission is 2.6×10^{-4} s^{-1}).[9] In compressed gas and in solution the transition probability increases by 3–4 orders of magnitude; luminescence is detected using sensitive photomultipliers.[14,17,53,56] Such a luminescence was first detected in solutions of biological pigments (photosensitisers of $^1O_2$) using an improved phosphoroscope under steady-state excitation.[14,60] Later on, the characteristic narrow band at 1270 nm corresponding to the $a^1\Delta_g \rightarrow X^3\Sigma_g^-$ transition of oxygen molecule in solution was observed in numerous studies using pulsed excitations of photosensitisers.[1,17,58,61–64,73–77] Good temporal resolution obtained with a germanium detector was reported.[61–63,75] The quantum yield (Q_a) of luminescence ($a \rightarrow X$ transition) and the lifetime of singlet oxygen (τ_Δ) in some solutions of saturated hydrocarbons and their halo derivatives were measured.[63] Measurements of Q_a in the near IR region are complicated by the lack of appropriate references, because the quantum yield of singlet oxygen (Q_Δ) should be measured for each solution with a given sensitiser. The radiative rate constant for the $a^1\Delta_g \rightarrow X^3\Sigma_g^-$ transition [63]

$$k_{a-X} = \frac{Q_a}{\tau_\Delta Q_\Delta}, \tag{15}$$

determined for a series of saturated solvents falls in the range $\sim 0.1-0.2$ s^{-1}. The conclusion about independence of k_{a-X} on the solvent is only valid for this series of solutions.[63]

The author of this review developed [12,27,28] a simple scheme of stealing the emission intensity of the $a \rightarrow X$ transition of collision complexes of O_2 with diamagnetic molecules starting from calculations of a model complex $O_2 + H_2$. Using a program of configurational interaction calculations [12,97] for single and double excitations debugged for the modified [12] MINDO/3 method,[15] qualitatively correct description of the spectrum of the complex was obtained and the collision-induced electric dipole moments of transitions were calculated.[27,28] It was established that the $b-a$ transition of the collision complex acquires a relatively large dipole moment [see Eqn (13)]. As mentioned above, this is characteristic of all collisions of the O_2 molecule with diamagnetic molecules; this also follows from Eqns (13) and (14). In the case of a planar symmetric complex similar to that shown in Fig. 3, relation (13) predicts that the intensity of the $b-a$ transition of the O_2 molecule in the collision complex should dramatically increase due to deformation of the $\pi_{g,x}$-orbital electron cloud. Even small contributions of the collision-partner (H_2, N_2, C_2H_4, C_6H_6) orbitals induce a large dipole moment of the $b-a$ transition. With allowance for the abnormally strong spin–orbit coupling of the $b^1\Sigma_g^+$ and $X^3\Sigma_{g,0}^-$ states [see Eqn (8)] and for the contribution of the $|b^1\Sigma_g^+\rangle$ state to the wave function $\Psi_{X,0}$ of the ground-state term [see Eqn (10)] one gets that the $a^1\Delta_g \rightarrow X^3\Sigma_{g,0}^-$ transition 'steals' the intensity [12] from the $a-b$ transition

$$\langle a^1\Delta_g|D|\Psi_{X,0}\rangle = -c\langle a^1\Delta_g|D|b^1\Sigma_g^+\rangle. \tag{16}$$

Since the spin–orbit coupling (8) in the oxygen molecule is still the strongest and the coefficient c only depends on the properties of the O_2 molecule, the $|c|$ value in the collision complex remains almost unchanged.[27,98] The electric dipole moment of the $a^1\Delta_g - b^1\Sigma_g^+$ transition of the collision complex $O_2 + H_2$ at $R = 2.4$ Å is [28]

$$\langle a^1\Delta_g|D|b^1\Sigma_g^+\rangle = 0.0113 \text{ e Å}.$$

The moment of the $O_2 + H_2$-collision induced transition $a^1\Delta_g \rightarrow X^3\Sigma_{g,0}$ determined using relation (16) is

$$\langle a^1\Delta_g|D|\Psi_{X,0}\rangle = 1.5\times10^{-4} \text{ e Å},$$

which corresponds to an absorption oscillator strength f of 2×10^{-9} and a radiative rate constant of $k_{a-X} = 0.08$ s^{-1}. This coincides in order of magnitude with the results obtained by Krasnovsky [63] ($k_{a-X} \approx 0.1$ s^{-1}). The electron shell of the H_2 molecule provides a simple example of the closed electron shell of the molecule of a saturated compound; therefore, the model for the $O_2 + H_2$ complex chosen here is quite reliable.[12,28] This was confirmed in calculations of O_2 complexes with other molecules.[43,53,54,71,84–88,109]

As mentioned above, the Noxon band enhancement depends on the polarisability of the collision partner, which leads to the same dependence for the luminescence band $a^1\Delta_g \rightarrow X^3\Sigma_g^-$. The dependence of the radiative rate constant k_{a-X} on solvent properties has been a subject of discussion initiated by the contradictory results of measurements using different luminescent standards for calibration.[1,17,35,36,60–64,73–77,101–106] Ogilby *et al.* [17,77,104] showed that the relative rate constant k_{a-X} changes by an order of magnitude on going from trifluoroethanol to carbon disulfide. These discussions outcompeted a problem of paramount importance, namely, why the intensity of the spin-forbidden transition $a^1\Delta_g \rightarrow X^3\Sigma_g^-$ increases by 3–4 orders of magnitude upon collisions in solutions, gases and solid matrices compared to the intensities of the transitions of free oxygen molecule.[27] The mechanism of stealing the intensity of this transition from the $a^1\Delta_g - b^1\Sigma_g^+$ transition of collision complexes was proposed more than two decades ago;[12,28] however, until recently [1,17,43,56] it attracted no attention of specialists in singlet oxygen photophysics. From relation (16) it follows [12,28] that the ratio of the rate constants for oxygen–solvent collision induced transitions,

$$\frac{k_{a-X}}{k_{b-a}} = \frac{\omega_{a-X}^3 D_{a-X}^2 g_X g_b}{\omega_{b-a} D_{b-a}^2 g_a^2} = \frac{3\omega_{a-X}^3|c|^2}{4\omega_{b-a}^3} = \tag{17}$$

$$= \frac{3(7882\,\text{cm}^{-1})^3|0.0134\text{i}|^2}{4(5239\,\text{cm}^{-1})^3} = 0.00045$$

(ω is the transition frequency) should be constant for any solvent, because collisions do not affect mixing of the states (10) and (11) due to SOC. Here, we accounted for equality

$$\langle a^1\Delta_g|D|b^1\Sigma_g^+\rangle = D_{a-b} = D_{b-a}$$

and used the statistical weights ($g_X = 3$, $g_a = 2$, $g_b = 1$). The matrix element of SOC (11) in oxygen molecule reaches the maximum possible value; its magnitude is large *per se* and does not need an increase through symmetry reduction upon collision. The latter is necessary for the singlet – singlet transition $a^1\Delta_g - b^1\Sigma_g^+$, which is symmetry-forbidden for isolated O_2 molecule in the dipole approximation; this prohibition is

effectively removed in collision complexes. Thus, the spin prohibition to the $a-X$ transition is removed due to the SOC in the O_2 molecule itself. This provides an explanation for an increase in the $a-X$ transition probability by three and more orders of magnitude in almost any solvent (in proportion to an increase in the $b-a$ transition probability).[12]

Pioneering studies [12, 28] in this field were devoted to explanation of the results obtained by Krasnovsky,[63] who investigated the luminescence of singlet oxygen in solutions. These studies attracted the attention of researchers who studied the spectra of O_2 in crystals of noble gases [51, 52] and in buffer gas mixtures.[39] Considerable enhancement of the $b \rightarrow a$ and $a \rightarrow X$ transitions was found for oxygen present in Ne, Ar, Kr and Xe matrices. The intensity increased with an increase in the atomic number of the noble gas.[51, 52] Gas-phase experiments gave the following values of the ratio (17): 0.00032 (Ne), 0.00037 (Ar), 0.00042 (Kr) and 0.00083 (Xe).[39] (The last value for Xe can be easily explained by additional enhancement of the singlet–triplet transition $a \rightarrow X$ due to the effect of the external heavy atom.[25, 98]) Similar values of the ratio (17) confirmed predictions of theoretical studies [12, 27, 28, 98] while a slight increase in this ratio with the noble gas atomic number was explained by the strengthening of the SOC and by the effect of the external heavy atom.[24, 25]

The ratio of the statistical weights of all states (17) was taken to be unity,[88] because the collision model chosen assumed only one sublevel of the a and X states is active in transitions. Indeed, only the sublevel (10) of the $X\,^3\Sigma_g^-$ state with the quantum number $M_S = 0$ is involved in the formation of the intensity of collision-induced transition $a \rightarrow X$ through 'mixing' with the $b^1\Sigma_g^+$ state and stealing of the dipole moment of the Noxon transition [see Eqn (16)]. Both components of the degenerate state $a^1\Delta_g$ can participate in the Noxon band enhancement [see Eqns (13) and (14)]; however, the total intensity corresponds to involvement of only one component (at least for most calculated models for complexes).[12, 27, 87, 88] Therefore, for the $b \rightarrow a$ transition the statistical weights of the states participating in the transition are equal to unity. Irrespective of the type of the system (gas or solution) and $O_2(a^1\Delta_g)$ generation procedure (gas discharge or sensitisation) both components of the Δ_g state are populated before light emission. Therefore, the statistical weight ratio of the lower-to-upper term for the $a \rightarrow X$ collision-induced transition is 1 : 2. Thus, the actual ratio of these quantities in relation (17) is 1/2 rather than 3/4 and theory predicts [88] that

$$\frac{k_{a-X}}{k_{b-a}} = \frac{\omega_{a-X}^3 D_{a-X}^2}{\omega_{b-a} D_{b-a}^2 g_a} = \frac{\omega_{a-X}^3 |c|^2}{2\omega_{b-a}^3} = 0.0003, \qquad (17a)$$

which corresponds to the results of measurements in gases,[39] solutions [1, 17, 64, 106] and cryogenic matrices.[51]

Analysis of the electronic emission spectrum of NCl molecule in Ar matrix[68] gave a clear substantiation of the theoretical model (9)–(14), (16). This molecule is a valence-isoelectronic analogue of oxygen molecule; it has a triplet ground state $X\,^3\Sigma^-$ and the same set of excited singlet states, $a^1\Delta$ and $b^1\Sigma^+$, as the O_2 molecule.[9] Nitrogen chloride molecule only possesses no inversion symmetry; therefore, electric dipole transitions $b \rightarrow X$ and $a \rightarrow X$ with inclusion of the SOC are allowed.[12, 42] In particular, the $a \rightarrow X$,1 transition is allowed for the sublevels with $M_S = \pm 1$, while transition to the $M_S = 0$ sublevel is forbidden, as well as the corresponding magnetic dipole transitions of free oxygen molecule.[12] The scheme of the $b \rightarrow a$ and $a \rightarrow X$ transition enhancement for the complex with Ar atom in an inert matrix is the same as that proposed for the O_2 collision complexes considered above [see Eqns (9)–(14)]. Only transition to the sublevel with $M_S = 0$ is enhanced, as follows from relation (16). The NCl molecule is convenient in that the zero-field splitting for sublevels of the $X\,^3\Sigma^-$ state is clearly seen [68] in the $a \rightarrow X$ emission spectrum. In addition to the allowed transition $a \rightarrow X$,1 the spectrum of NCl in Ar matrix (1091.2 nm) exhibits a weak band of the $a \rightarrow X$,0 transition (1090.7 nm), which is strictly forbidden for free molecule.[68] The change in the intensity of this band obeys relation (16) with the coefficient $c = 0.026$ for the NCl molecule (obtained by the author of this review from configurational interaction calculations with inclusion of SOC and with allowance for the measured probability of the $b \rightarrow a$ transition in the Ar matrix).[68]

The intensities of the $a \rightarrow X$,0 transitions of isovalent molecules NBr and NI in solid argon are also in agreement with the model (16). Analysis of the relative intensities in the fine structure of the $a^1\Delta \rightarrow X\,^3\Sigma_\Omega^-$ bands of the isoelectronic molecules NCl, NBr and NI in solid argon [68] confirmed the validity of the intensity borrowing theory for this band [see Eqns (8)–(13)], considered taking oxygen as an example. These data, which were obtained long before the results of direct intensity measurements for the $b \rightarrow a$ and $a \rightarrow X$ transitions of oxygen in solutions,[17, 64] provided strong arguments in favour of correctness of the model (8)–(13), (17a). However, for a decade did these data remain uncalled by researchers who studied photophysics of the singlet state of oxygen in organic and biological systems.[43, 61–64]

In the late 1990s Schmidt *et al.*[1, 64] and Ogilby [17] carried out direct experimental evaluation of theoretical predictions made using relation (17) for certain solutions. For liquid CCl_4 at room temperature the ratio of the rate constants $k_{a-X} = 1.1\ s^{-1}$ and $k_{b-a} = 3400\ s^{-1}$ is 0.000325, which is similar to the value 0.00317 obtained in the argon matrix ($k_{a-X} = 0.013\ s^{-1}$ and $k_{b-a} = 41\ s^{-1}$ at 5 K).[1, 51, 64, 106] In spite of large differences between the rate constants, the ratio (17a) also remains constant for some other solutions.[17, 64] This ratio was measured [82] for the absorption of singlet and triplet oxygen molecules in deuterated water, where $O_2(a^1\Delta_g)$ has a relatively long lifetime. In all cases including homogeneous mixtures of solvents the $a-X$ and $b-a$ transition probabilities changed in parallel, as predicted by theory.[12, 27]

Knowledge of the enhancement mechanism of the radiating capacity of singlet oxygen is crucially important for progress in photobiology and medicine. Detection of $O_2(a^1\Delta_g)$ in various biological media is difficult owing to weak intensity and low temporal resolution of the $a \rightarrow X$ phosphorescence signals [this is determined by the radiative rate constant that strongly depends on the structure of (i) biopolymers in the oxygen environment and (ii) entire solution]. Singlet oxygen plays an important role in photobiological processes and photodynamic therapy;[1, 17, 18] therefore, one can expect that *in vivo* detection of $O_2(a^1\Delta_g)$ will become a tool of medical practice in the near future. The widely used procedure for $O_2(a^1\Delta_g)$ detection with cryogenic germanium diodes is still far from meeting these requirements. The use of modern photomultipliers for the near IR region (sensitivity of these devices at 1270 nm is ten times higher than that of germanium diodes) allowed the lifetime of $O_2(a^1\Delta_g)$ to be measured ($\tau_\Delta = 40$ ns, $Q_\Delta = 0.005$) *in vivo* in rat liver studies.[1] Biological media are highly inhomogeneous and the observed lifetime of singlet oxygen is the average result of various quenching processes. Note that the τ_Δ values are many orders of magnitude smaller than the radiative lifetimes τ_Δ^r determined from the rate constants $k_{a-X} = 1/\tau_\Delta^r$. However, understanding of the mechanisms of intermolecular interactions responsible for the τ_Δ^r values is at least equally important for progress in theory and strategy of $O_2(a^1\Delta_g)$ detection compared to the understanding of quenching mechanisms.

As mentioned above, the rate constant k_{a-X} increases in proportion to the increase in the rate constant k_{b-a} upon

collision of O_2 with the solvent molecule M.† The latter constant depends on the difference between the induced dipole moments of two degenerate MOs, $\pi_{g,x}$ and $\pi_{g,y}$ [see Eqn (13)] and, hence, on the polarisability of the solvent molecule α_s. Such an asymmetry of charge transfer to these orbitals of oxygen molecule appears in the case of a 'planar' collision, where the O_2 and M molecules lie in the same plane or where the atomic orbitals of the nearest atoms in the O_2 and M molecules overlap to the greatest extent and share the nodal plane. Deviation from this 'planar' structure causes mutual cancellation of both terms in relationship (13), but this is accompanied by an increase in the summands in expression (14). All summands in Eqns (13) and (14) depend on the overlap of the O_2 and M molecular orbitals and on the orbital mixing. Intermolecular interaction responsible for an increase in the rate constant k_{a-X} is essentially dispersion interaction,[12, 88] and depends on R^{-6}. The polarisability of the solvent molecule can be expressed through molar refraction:[64]

$$R_m = \frac{4\pi}{3} N_A \alpha_s ,$$

where N_A is the Avogadro constant.

If the interaction responsible for acceleration of the $a \rightarrow X$ transition is bimolecular in character, the second-order rate constant

$$k^c_{a-X} = \frac{k_{a-X}}{[S]} \qquad (18)$$

should be related to the molar refraction ([S] is the molar concentration of solvent). Actually, linear correlations between $\log k^c_{a-X}$ and $\log R_m$ were observed for a large number of solutions.[64] The radiative rate constants for $a \rightarrow X$ phosphorescence corresponding to neat liquids are listed in Table 1. The k_{a-X} vary over a wide range from 0.209 s^{-1} for water to 3.14 s^{-1} for CS_2.

The first-order rate constants k_{a-X} were calculated assuming [12, 27] that the whole solvent is represented by the nearest collision-partner and the lifetime of such a complex in the solvation shell is sufficiently long to determine the rate constant.

The effect of solvent was also included in other models.[12, 27, 54, 71, 85, 86, 99] For instance, a loosely bound collision complex O_2 + M was placed in a solvent cavity; the solvent was treated as dielectric continuum (semi-continuum model).[71] Short-range interactions in the O_2 + M pair are fundamentally important for the description of quantum exchange and dispersion interactions responsible for the enhancement of quantum transitions and shifts of energy levels. The semi-continuum model allows for small additional corrections to transition energies, which leads to better agreement between experimental data and results of bathochromic shift calculations‡ for the $a \rightarrow X$ transition band in solutions; however, the effect of continuum on the emission intensity is negligible.[54, 71] The 0–0 transition band in the gas phase (7882 cm^{-1}, see Ref. 9) is slightly shifted in trifluoroacetic acid (7873 cm^{-1}), the shift being more pronounced in other solvents (*e.g.*, CH_2I_2: 7824 cm^{-1}).[1] A bathochromic shift of the $a \rightarrow X$ transition band within 100 cm^{-1} was predicted in the first calculations of O_2 + M complexes with M = H_2, C_2H_4, C_6H_6, $C_{10}H_8$.[12, 103] *Ab initio* calculations [71] gave a 45 cm^{-1} shift (see Table 3 in Ref. 71) for the 0–0 band of the $a^1\Delta_g \rightarrow X^3\Sigma_g^-$ transition of oxygen in benzene, which is in agreement with experimental data.[1, 54] The calculated dependence of the bathochromic shift of the $a \rightarrow X$ transition band in the collision complex O_2 + Ar on the interparticle distance was reported;[98] the shift is very small ($\Delta\nu$ = 2.1 cm^{-1}) near the potential curve minimum (R = 3.6 Å) and rapidly increases as R decreases. At R = 3.25 and 3 Å, where the repulsive potential considerably increases, one gets $\Delta\nu$ = 13.2 and 39 cm^{-1}, respectively. The continuum model of self-consistent reactive field of the solvent gives poorer results.[71] This model ignores the overlap and orbital mixing between the collision partners, which precludes correct calculations of not only enhancement of the radiating capacity of the $a \rightarrow X$ transition, but also the solvatochromic shift.

Knowledge of the enhancement mechanism of singlet oxygen radiating capacity is also basic to understanding of the nature of solvatochromic shift of the $a-X$ band. In all solutions studied the maximum of the 0–0 phosphorescence band of O_2 (7882.4 cm^{-1}) is shifted by 20–50 cm^{-1} towards the long-wavelength region, the shift increasing with the solvent polarisability.

Taking into account the fact that the major contribution to the shift of energy levels comes from dispersion interaction, Schmidt [1, 35] proposed a theory of solvatochromic shift of the $a-X$ band. The theory assumes that the shift of the maximum of the 0–0-band ($\Delta\nu$) depends on the polarisability difference between the $a^1\Delta_g$ and $X^3\Sigma_g^-$ states (*i.e.*, on α_Δ and α_Σ)

$$\Delta\nu = -\frac{3\alpha_s}{2d_c^6}\left(\frac{\alpha_\Delta I_\Delta I_s}{I_\Delta + I_s} - \frac{\alpha_\Sigma I_\Sigma I_s}{I_\Sigma + I_s}\right),$$

where I_Σ, I_Δ and I_s are the ionisation potentials of the O_2 and solvent molecules, $d_c = (d_\Sigma + d_s)/2$ is the distance between spherical molecules, d_s is determined from the molar volume of

Table 1. Radiative rate constants for singlet–triplet transition $a^1\Delta_g \rightarrow X^3\Sigma_g^-$ of oxygen molecule in different solvents.[17, 64, 76, 74, 104]

Solvent	k_{a-X}/ s^{-1}	k^c_{a-X}/ litre mol^{-1} s^{-1}
Water	0.209	0.0038
Methanol	0.390	0.0159
Acetonitrile	0.45	0.0234
Acetone	0.543	0.040
Ethanol	0.55	0.032
Cyclohexane	0.66	0.071
Chloroform	0.962	0.077
Tetrachloromethane	1.17,[a] 0.8,[b] 0.25[c]	0.113
Toluene	1.44	0.153
Benzene	1.50[a]	0.133
Chlorobenzene	1.68	0.171
Tetrachloroethylene	1.89	0.193
Iodobenzene	2.61	0.291
Diphenyl sulfide	2.66	0.442
1,3-Dibromobenzene	2.72	0.328
1-Methylnaphthalene	2.96	0.420
1-Bromobenzene	3.11	0.432
Carbon disulfide	3.14	0.189

Note. k_{a-X} and k^c_{a-X} are the mono- and bimolecular rate constants, respectively. For free O_2 molecule (*in vacuo*),[1, 9] k_{a-X} = 0.00023 s^{-1}. For a homogeneous mixture of solvents $k_{a-X} = \sum_i k^c_{a-X,i}[i]$, where $[i]$ is the molar concentration of the ith component of the system and $k^c_{a-X,i}$ is the corresponding second-order rate constant.

[a] Measured using three different sensitisers with their fluorescence as luminescence standards.[64]

[b] With Li–Nd phosphate glass as luminescence standard.[101]

[c] With fluorescence of tetraphenylporphine as luminescence standard.[63]

† Notations: M is the solvent molecule involved in the collision complexes and S are other solvent molecules.

‡ Shift towards long-wavelength region.

the solvent and d_Σ is determined from the van der Waals volume of the O_2 molecule. The solvent polarisability

$$\alpha_s = \frac{3R_m}{4\pi N_A}$$

was determined through the refraction

$$R_m = V_m P_n ,$$

where V_m is the molar volume of the solvent,

$$P_n = \frac{n^2 - 1}{n^2 + 2},$$

(n is the refractive index). To explain the bathochromic shift of the $a-X$ band, Schmidt assumed [35] that $\alpha_\Delta > \alpha_\Sigma$, as is the case for the excited-state and ground-state polarisabilities. However, the characteristics of the open-shell oxygen molecule [see Eqns (1)–(3)] and the paramagnetic ground state are basically different from those of conventional diamagnetic molecules with closed shells in the ground state. This also concerns the polarisability tensor. For instance, the diagonal elements of this tensor for the x axis are defined as follows:

$$\alpha_{xx} = \sum_n \frac{\langle 0|ex|n\rangle\langle n|ex|0\rangle}{E_n - E_0}, \qquad (18a)$$

where ex is the projection of the dipole moment on the x axis; $|n\rangle$ and E_n are respectively the wave function and energy of the nth excited state; the case $|n\rangle = 0$ (not included in the sum) corresponds to the ground state for which the tensor is calculated.[13] Expressions for other components of the tensor are similar. The excited-state polarisability of a conventional organic molecule should be higher than that of the singlet ground-state, because the energies of transitions between excited states are always lower than the energy of excitation from the closed shell at a sufficiently large number of intense transitions in both cases.

Schmidt's assumption [35] $\alpha_\Delta > \alpha_\Sigma$ was rejected based on the results of *ab initio* calculations of O_2 molecule (see Refs 40, 53 and 93), which also cast some doubt [53] on his theory of red solvatochromic shift of the $a-X$ band. At all values of the internuclear distance in the O_2 molecule, the polarisability in the $a^1\Delta_g$ state is lower than in the $X^3\Sigma_g^-$ state,[98] which contradicts the Schmidt hypothesis. Thus, even averaging over vibrational states does not change the conclusion, namely, $\alpha_\Delta < \alpha_\Sigma$. This result can be explained as follows. The polarisability α_Σ of the triplet ground state is mainly determined by the electric dipole moment of the Schumann–Runge transition (D_{SR}^2, divided by the transition energy), whereas that of the singlet state $a^1\Delta_g$ is determined by the electric dipole moment of the $a^1\Delta_g - {}^1\Delta_u$ transition, which is much smaller than D_{SR} (Schumann–Runge transition energy is also lower, especially at $r > 1.23$ Å).[30, 66] Here the case in point are the components of the tensor α_{zz}, since these transitions are polarised along the molecular axis. It is these transitions that make the major contributions to the average polarisability

$$\alpha_{cp} = \frac{2\alpha_{xx} + \alpha_{zz}}{3}.$$

The perpendicular component is determined by the dipole moments of transitions to the ${}^{1,3}\Pi_u$ states, which are nearly equal for the triplet and singlet transitions. The α_{xx} and α_{zz} values we have obtained are respectively 8.16 and 15.48 a_0^3 for the $X^3\Sigma_g^-$ state and 8.15 and 14.12 a_0^3, respectively, for the singlet state $a^1\Delta_g$. Here $\alpha_{cp} = 10.6\, a_0^3$ for $X^3\Sigma_g^-$ and $\alpha_{cp} = 10.14\, a_0^3$ for $a^1\Delta_g$, $\alpha_\Delta - \alpha_\Sigma = -0.46\ a_0^3$.

The relation $\alpha_\Delta < \alpha_\Sigma$ is valid for free O_2 molecule in vacuum,[53] but will it hold for oxygen in solution? To clarify the issue, we carried out polarisability calculations for collision complexes of O_2 with diamagnetic molecules.[98] As an example we will consider a collision complex O_2 + He, where the He atom serves a model for a simplest closed-shell species.[98] In this case the average polarisabilities of the triplet and singlet states somewhat increase to $\alpha_{cp} = 11.72\, a_0^3$ for $X^3\Sigma_g^-$, $\alpha_{cp} = 12.69\, a_0^3$ for $a^1\Delta_g$, *i.e.*, $\alpha_\Delta > \alpha_\Sigma$. The reason consists in the appearance of additional contribution to polarisability due to the induced $a-b$-transition [see Eqns (13) and (14)] and the contributions of charge transfer transitions for the $a^1\Delta_g$ state. The charge transfer transitions are more intense for the $a^1\Delta_g$ state rather than $X^3\Sigma_g^-$ ground state.[12, 27 70] The singlet and triplet charge transfer states are almost degenerate;[27] therefore, the energies of the charge transfer transitions from the singlet state $a^1\Delta_g$ are nearly 1 eV lower than those of similar transitions from the triplet ground state $X^3\Sigma_g^-$. The mixing coefficients of the triplet and singlet ground-state wave function (2) with the wave functions of the charge transfer states due to configurational interaction are noticeably larger for the $a^1\Delta_g$ state than for the $X^3\Sigma_g^-$ state,[12, 27] which predetermines higher intensities of dipole transitions and their greater contribution to polarisability.[98] The calculated polarisability difference

$$\alpha_\Delta - \alpha_\Sigma = 0.97\ a_0^3$$

is in qualitative agreement with the predicted value.[35] Using the results of such calculations, one can explain the red solvatochromic shift of the $a-X$ transition band in the framework of the Schmidt theory.

Thermal motion of molecules in solutions is reduced to random jumpwise translational motions from one metastable position to another. O_2-Type gas molecules are known to exist in solutions in cavities, with rather long lifetimes that are much longer than the jump time. An important contribution to stimulation of the radiative transition $a^1\Delta_g \to X^3\Sigma_g^-$ of oxygen molecule comes from asymmetrical intermolecular vibrations in those cavities that are included in modelling as the effect of nearest neighbours only. The inclusion of a few solvent molecules in the nearest solvation shell leads to non-additive enhancement of the $a \to X$ transition.[98] Model ternary complexes $O_2 + C_2H_4 + H_2$ were calculated[100] at different collision geometries and co-operative effects of a complex solvation shell on the intensities of the $b \to a$ and $a \to X$ transition bands were studied in detail. It was shown that both an increase and a decrease in the probability of the radiative transition $a \to X$ are possible depending on the mutual position of the collision partners. By and large, calculations [98, 100] revealed the possibility of co-operative effect of a few solvent molecules on the moment of the $a \to X$ transition, which explains a large enhancement of singlet oxygen emission in solution compared to that observed in the gas phase.

Fink *et al.*[39] studied the intensity of the Noxon band in the microwave discharge spectra of O_2 mixtures with noble and other gases at a reduced pressure. Using a FT IR spectrometer, they obtained a high resolution for the $b \to a$ transition band at 1.91 μm and found that raising the pressure causes the appearance of a continuum against the background of discrete lines of rotational branches of the $b^1\Sigma_g^+ \to a^1\Delta_g$ quadrupole transition. The discrete spectrum was assigned[39] to unperturbed $O_2(b^1\Sigma_g^+)$ molecule, while the continuum was attributed to collision-induced emission. Metastable molecules $O_2(b^1\Sigma_g^+)$ generated in discharge also give rise to an emission band $b^1\Sigma_g^+ \to X^3\Sigma_g^-$ the intensity of which depends only slightly on collisions.[39] This follows from the old semiempirical theory [12, 25] and is confirmed by *ab initio* calculations,[87] namely, with allowance for the SOC [see Eqns (9) and (10)] the electric dipole moment of the $b \to X$ transition is proportional to the dipole moment

Table 2. Radiative rate constants for singlet–singlet transition $b^1\Sigma_g^+ \rightarrow a^1\Delta_g$ of O_2 molecule induced by collisions with various buffer gas molecules.[39]

Buffer gas	k^c_{b-a}/ litre mol^{-1} s^{-1}	R_m/ ml mol^{-1}
He	$\leqslant 0.6$	–
Ne	~ 0.6	1.00
N_2	7.8	4.34
O_2	9.0	4.00
Ar	10.2	4.13
Kr	21.6	6.22
Xe	46.8	10.10
SF_6	26.4	11.34
SO_2	31.8	9.71
PCl_3	252.0	25.0

Note. Bimolecular constants k^c_{a-X} were determined from the integral intensity ratio of discrete lines and broad bands corresponding to collision-induced transitions. The rate constant for the $b^1\Sigma_g^+ \rightarrow a^1\Delta_g$ transition of free O_2 molecule was taken to be $k_{b-a} = 0.0014$ s^{-1} (Ref. 39).

difference between the $b^1\Sigma_g^+$ and $X^3\Sigma_g^-$ states. For some calculated collision complexes this difference is negligible and no $b \rightarrow X$ transition enhancement is observed.

Once measured the intensity ratios of the $b \rightarrow X$ and $b \rightarrow a$ transition bands as functions of pressure of various gases, the second-order rate constants for collision-induced singlet–singlet transition $b \rightarrow a$ (Table 2) were determined.[39] For neon, one has $k^c_{b-a} = 0.9 \times 10^{-21}$ cm^3 s^{-1}, whereas for PCl_3 this rate constant increases by a factor of 467 ($k^c_{b-a} = 42 \times 10^{-20}$ cm^3 s^{-1}).[39] In Table 2 the rate constants taken from Ref. 39 are given per mole in order to compare with the results of measurements in solutions.[1] The rate constants for quenching of excited $O_2(b^1\Sigma_g^+)$ molecules are 2–3 orders of magnitude higher than the radiative rate constants in the gas phase.[1, 39] In the condensed phase quenching is even more efficient; therefore, luminescence measurements for the $b \rightarrow a$ transition in solutions are difficult.[1, 17, 58, 64] Chou and Frei [58] first discovered this emission in CCl_4 solution using triplet benzophenone as sensitiser of the $O_2(b^1\Sigma_g^+)$ state. This result could not be reproduced for long.[106] Taking into account the low rate constant for the Noxon band in free O_2 molecule ($k_{b-a} = 1.4 \times 10^{-3}$ s^{-1}), the observation of a narrow band at 1.92 μm indicated [58] a giant enhancement of the $b \rightarrow a$ transition in solution. According to Schmidt *et al.*,[1, 106] the quantum yield of luminescence for the $b \rightarrow a$ transition in CCl_4 solution is 0.00045. Using the observed lifetime of $O_2(b^1\Sigma_g^+)$ molecules, he determined the radiative rate constant for the Noxon band in CCl_4 solution ($k_{b-a} = 3.45 \times 10^3$ s^{-1}); this is six orders of magnitude higher than the rate constant for free O_2 molecule. The calculated moment of the $b \rightarrow a$ transition in the collision complex $O_2 + CCl_4$ depends strongly on the intermolecular distance, being almost independent of collision angles.[12] The average value of R is governed by the molecular velocity in the vicinity of the nearest solvation shell. Assuming that $R_{av} = 2.87$ Å at room temperature, one can obtain the observed enhancement of the $b \rightarrow a$ transition. Tetrachloromethane is not a 'champion' with respect to enhancement of the $a \rightarrow X$ and $b \rightarrow a$ transitions in solutions, as follows from calculations [12, 24–28, 85–88, 98–100] and from the data listed in Table 1.

3. Inclusion of vibrations and vibronic interactions

Enhancement of forbidden transitions in oxygen molecule trapped in a low-temperature inert gas matrix is much less pronounced.[98–123] Taking into account the symmetry of the nearest environment of an impurity O_2-centre in the crystal lattice, one can conclude that the $b \rightarrow a$ transition remains forbidden ignoring lattice vibrations.[113, 123] Transitions become allowed only when assisted by electron–phonon interactions.[123] In argon matrix at 5 K, the $b \rightarrow a$ transition is characterised by a radiative lifetime of 24.5 ms, or a rate constant $k_{b-a} = 41$ s^{-1} (Refs 51 and 52), which is nearly two orders of magnitude lower than in CCl_4 solution. In this matrix the electric dipole moment of the $b \rightarrow a$ transition is induced by each neighbouring argon atom, in the direction from O_2 towards Ar, so the resultant moment of the transition is zero. Thus, enhancement of the $b \rightarrow a$ transition can be due to asymmetrical lattice vibrations. With allowance for nuclear displacements

$$q = R - R_0$$

from the equilibrium position R_0 (change in the intermolecular distance) in the adiabatic approximation, the dipole moment of a vibronic transition $a \rightarrow X$ can be written in the form [113]

$$\langle a^1\Delta_g\chi_0 | D | \Psi_{X,0}\chi_v \rangle = -c\left(\frac{\partial D_{b-a}}{\partial q}\right)_{R_0} \langle \chi_0 | q | \chi_v \rangle, \qquad (19)$$

where χ_0 and χ_v are the vibrational functions with quantum numbers 0 and v, respectively; for the coefficient c, see Eqn (11). By analogy, for the $b \rightarrow a$ transition one gets

$$\langle b^1\Sigma_g^+\chi_0 | D | a^1\Delta_g\chi_v \rangle = \left(\frac{\partial D_{b-a}}{\partial q}\right)_{R_0} \langle \chi_0 | q | \chi_v \rangle.$$

The equilibrium positions and vibrational functions for the states b, a and X are thought to be the same, which is quite realistic.[9, 98] For many models the calculated moment of the D_{b-a} transition depends strongly on q near the equilibrium complex $O_2 + M$.[12, 98, 99, 113] The radiative rate constants for the $a \rightarrow X$ and $b \rightarrow a$ transitions determined with allowance for asymmetrical vibrations in the octahedral model of impurity centre $O_2 \cdot Ar_6$ are similar to the observed ones.[12, 51, 98]

The 0–0-bands of the $a \rightarrow X$, $b \rightarrow a$ and $b \rightarrow X$ transitions are the most intense because the potential curves for these states are characterised by nearly equal equilibrium distances (see Fig. 1). The Franck–Condon (FC) factors for these bands approach unity, whereas for vibronic overtones they are negligible. For O_2 in the gas phase, even the 0–1 bands have low intensities. In addition to the FC factors, here the dependence of the transition moment on the interatomic distance r should also be taken into account. The magnetic moment of the transition [see expression (12)] rapidly increases with the distance r, because the energy difference in the denominator of Eqn (11) decreases to zero in the limit $r \rightarrow \infty$. The Einstein coefficients for spontaneous emission of this transition determined by integration over r for the magnetic moment of the $b \rightarrow X$ transition of O_2 molecule are equal to 0.0047, 0.0064 and 0.0003 s^{-1} for the 0–1, 1–0 and 2–0 bands, respectively.[50] These values are similar to measured ones [9] and their ratios differ from the FC factor ratios.

Deviations from the FC effects were also obtained for the $a \rightarrow X$ transition.[12, 86] In addition to the 0–0-band of the $a \rightarrow X$ transition (1.27 μm), Chou and Khan [114] found a new, very weak emission band near 1.4 μm in spectra of chlorine-containing organic solvents ($C_2H_4Cl_2$, $C_3H_5Cl_3$, *etc.*). The band is red-shifted relative to the 0–0-band, the shift being equal to the C–Cl vibrational frequency. Similar weak bands were also detected for other halogen-containing solutions.[114] They correspond to the $a \rightarrow X$ transition of O_2 and simultaneous vibrational excitation of the solvent molecule.

Understanding of the nature of these co-operative vibronic transitions is of fundamental importance for theory of singlet state ($a^1\Delta_g$) of oxygen in solutions. Having included these transitions, one can obtain direct substantiation of relations

(11) and (16) and the bimolecular model for oxygen complex with solvent as the primary source of stimulation of emission of the forbidden transition $a^1\Delta_g \rightarrow X\,^3\Sigma_g^-$ (Ref. 113).

A model for the complex of O_2 with CH_3Cl used in calculations [113] of the transition moment D_{b-a} and its derivative [see Eqn (19)] is shown in Fig. 4. The dipole moment of cooperative vibronic transition $a \rightarrow X$ with simultaneous vibrational excitation of the C–Cl bond in CH_3Cl molecule can be calculated using expression (19) and the standard integral

$$\langle \chi_0 | q | \chi_{v=1} \rangle = \sqrt{\frac{\hbar}{2\mu\omega}},$$

where μ is the reduced mass and ω is the vibration frequency.

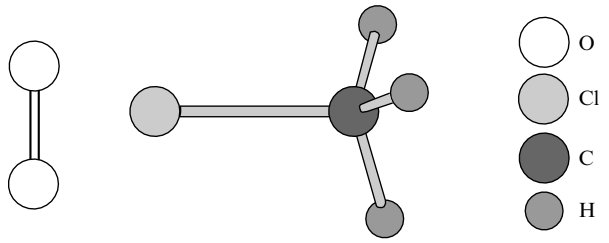


Figure 4. Structure of a collision complex $O_2 + CH_3Cl$. C–Cl vibration modulates the intermolecular distance in the equilibrium complex.

Vibrations of the C–Cl bond in the equilibrium complex modulate the intermolecular distance, which in turn strongly affects the moment of the $a \rightarrow X$ electronic transition, induced by intermolecular interactions. The dipole moment of cooperative vibronic transition [see Eqn (19)] was estimated to be equal to 1.42×10^{-5} e Å.[113] This leads to a radiative rate constant of 0.0056 s^{-1}, which is nearly 100 times lower than typical rate constants for the a–X transition of the O_2 molecule in related solvents (see Table 1). This estimate is in good agreement with the results reported by Chou and Khan:[114] the new emission band is about 100 times less intense than the 0–0-band of the $a \rightarrow X$ transition.

Absorption of thermal IR radiation by homonuclear molecules O_2 and N_2 is strictly forbidden by selection rules. However, weak absorption of IR radiation by air at 6.4 μm is known. Theory of intensity of vibrational transitions is intimately connected with the theory of enhancement of absorption bands of oxygen in electronic spectra. Geometry optimisation of O_2 + Ar complexes allowed the shifts of the IR bands in different excited states of the O_2 molecule and the corresponding band intensities to be calculated. Of particular importance is the theoretical prediction, [98] according to which intermolecular interaction affects the $O_2(^5\Pi_g)$ metastable state and its IR absorption spectrum. This state is formed upon recombination of $O(^3P)$ atoms in atmosphere and corresponds to a loosely bound complex or a biradical pair $O(^3P)\cdots O(^3P)$ with a long internuclear distance (2.2 Å). The bond energy (0.12 eV) and vibrational frequency (113 cm^{-1}) of this species are unexpectedly low for diatomic molecule.[98] Recently,[94] this associate was detected by the quintet–quintet transition to the ion-pair state. According to calculations of the complex O_2 + Ar, it is the $^5\Pi_g$ state that is characterised by the greatest enhancement of IR absorption.[98] Loosely bound molecules O_2^* can 'stick' to inert gases or aerosol particles, which should manifest itself in the IR spectra. Recombination of $O(^3P)$ atoms also leads to formation of more stable states $^1\Sigma_u^-$, $^3\Delta_u$, $^3\Sigma_u^+$ of O_2^* molecules; this is accompanied by release of energy and subsequent decomposition of the complex of oxygen with aerosol. Only metastable quintets can readily relax, being at the same time bound to the third particle (aerosol). Check-up of these predictions seems to be important for remote control in atmospheric photochemistry.

4. Optical effects stimulated by collisions of oxygen and organic dye molecules

Among numerous optical effects,[1,2] we will consider the enhancement of absorption intensity upon $S_0 \rightarrow T_1$ transition of dye, quenching of dye luminescence and a number of cooperative transitions.[27,69–71,73–88,98–122] Organic dye molecules typically contain an extended π-conjugation chain and readily excitable π-electrons and have low triplet-state energies and high polarisabilities.[2,7] Therefore, the effects of intermolecular interaction manifest themselves most pronouncedly when they influence the optical properties of both oxygen and dye molecules. A collision between excited dye molecule and $O_2(^3\Sigma_g^-)$ produces a short-lived collision complex with a nearly zero equilibrium constant.[7,13] Mixing of excited states of the complex and electronic-vibrational relaxation can lead to quenching of fluorescence of the $S_1 \rightarrow S_0$ transition of the dye molecule [2,7,13]

$$S_1 + {}^3O_2 \longrightarrow T_1 + {}^3O_2, \quad (20)$$

$$S_1 + {}^3O_2 \longrightarrow T_1 + {}^1O_2\,(a^1\Delta_g \text{ or } b^1\Sigma_g), \quad (21)$$

$$S_1 + {}^3O_2 \longrightarrow S_0 + {}^1O_2\,(a^1\Delta_g \text{ or } b^1\Sigma_g). \quad (22)$$

Here S_0 and S_1 are the ground and excited singlet state of the dye molecule, respectively.

Measurements of the yield of T_1 triplet states of pyrene and anthracene molecules and its perfluoro analogues showed [2] that quenching of fluorescence proceeds by reaction (20); no energy-transfer products [see Eqn (21)] were detected. It has long been known [2] that the rate of fluorescence quenching by oxygen varies insignificantly on going from organic molecules [in this case the S_1-T_1 splitting is such that reaction (21) is exothermic] to molecules for which reaction (21) is highly endothermic. Reaction (22) is spin forbidden. Immediate quenching

$$S_1 + {}^3O_2 \longrightarrow S_0 + {}^3O_2$$

is independent of specific features of intermolecular interaction associated with paramagnetism of the oxygen, because there is no need of spin changes in individual molecules; this process should not differ from the quenching by conventional diamagnetic molecules and is therefore of low efficiency. At present, it is commonly accepted that quenching of dye fluorescence by oxygen is mainly due to stimulation of intersystem crossing (ISC) with the transition from the S_1 to the T_1 state.[1,2,13] Theoretical explanation for the high efficiency of ISC (20) is based on quantum chemical calculations of collision complexes.[27,70,71,103,109] Now we will give some examples including the results of recent calculations.[107]

First, we will consider a collision complex with ethylene as a simplified model. This unsaturated hydrocarbon is not a dye, but has the S_1- and T_1-states of the ππ*-type; calculations of the collision complex of ethylene with oxygen simulate the characteristic features of the intermolecular interaction of O_2 with the π-system. In this model the O_2 molecule is above the ethylene plane at the distance R between the centres of the molecules; the oxygen and carbon atoms form an equilateral trapezoid O–O–C–C similar to that formed by the oxygen and nitrogen atoms in the collision complex $O_2 + N_2$ (see Fig. 3). The complex was calculated [107] using the spin-restricted Hartree–Fock method for open-shell systems with inclusion of configuration interaction in the 6-311G** basis set. The active space of configuration interaction included the most important orbitals of oxygen (from $3\sigma_g$-MO to vacant

$3\sigma_u$-MO). Six ethylene orbitals were also included in the CI calculations.[107] The use of extended AO and CI basis sets made it possible to reach [107] a better accuracy compared to that reported earlier,[109] although the models of the complexes were identical.

Comparison of the results obtained by this method (Fig. 5) with the results of calculations of the moments of singlet–singlet transitions [109] showed that extension of the CI basis set leads to enhancement of certain collision-induced transitions. This first of all concerns the 1–4 transition (see Fig. 2), *i.e.*, the co-operative singlet–triplet transition of ethylene with simultaneous excitation of the oxygen $a^1\Delta_g$ state. This transition could be observed in emission as dye phosphorescence whose band is shifted towards the red spectral region by the energy of the $a^1\Delta_g - X^3\Sigma_g^-$ transition.[109] Simultaneously, collisions between oxygen and dye molecules cause quenching of dye phosphorescence; therefore, observation of this co-operative emission is difficult. In principle, it cannot be ruled out that appropriate choice of the dye and the solution concentration will allow one to detect this co-operative emission.

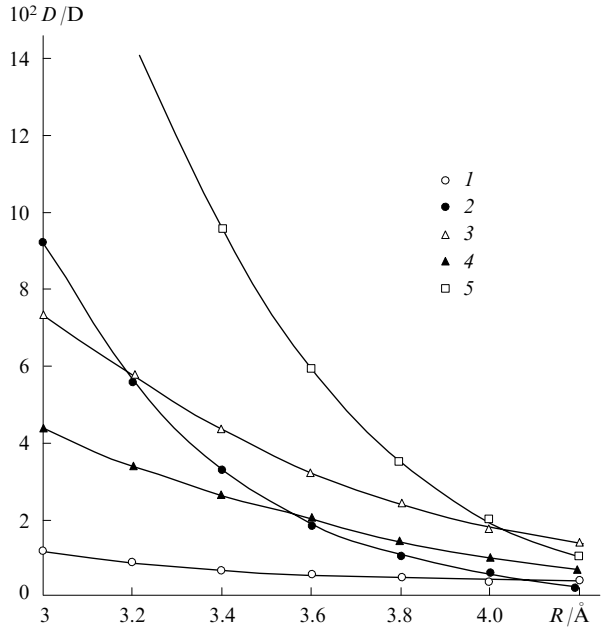


Figure 5. Dipole moments of singlet–singlet transitions (D) induced by collisions between oxygen and ethylene molecules plotted *vs.* intermolecular distance (R).
Calculations of configuration interaction with the 6-311G** basis set and molecular orbitals using the spin-restricted Hartree–Fock method. Transition (see Fig. 2): 3–1 (*1*), 1–4 (*2*), 1–5 (*3*), 3–2 (*4*) and 4–5 (*5*).

The dipole moment of the 1–4 transition rapidly decreases as R increases (see Fig. 5) and becomes the smallest among all dipole moments of the collision induced transitions at $R = 4.2$ Å. It is interesting to compare it with the dipole moment of the 1–5 transition ($a^1\Delta_g - c^1\Sigma_u^-$ transition of oxygen molecule, the frequency of which is similar to the frequency of the Chamberlain band $a^1\Delta_g - A'^3\Delta_u$).[94] The $a^1\Delta_g - c^1\Sigma_u^-$ transition with intensity strongly enhanced compared to those of the transitions of free oxygen molecule has been revealed in argon matrix;[108] this was explained by strong effect of intermolecular interaction on the electric dipole moment of this transition.[98, 107, 109] Figure 5 shows that the dipole moment of the 1–5 transition is large even at long intermolecular distances, being the largest among all calculated dipole moments at $R = 4.2$ Å. Enhancement of transitions for oxygen in inert gas matrix is determined by asymmetrical lattice vibrations relative to O_2; it depends on the difference between the distances to nearest neighbours rather than R. Therefore, enhancement of the $a^1\Delta_g - c^1\Sigma_u^-$ transition intensity at long intermolecular distances is of particular importance for explanation of the matrix effect on this transition.[109]

Comparison of two transitions, 1–5 and 1–4, shows that the latter becomes more intense at $R < 3.2$ Å (see Fig. 5). It was reported [109] that the dipole moments of the transitions increased not so rapidly, as shown in Fig. 5, as the molecules approached each other. This can be explained by lesser 'flexibility' of the 6-31G basis set (see Ref. 97) and poorer inclusion of electron correlation in the configuration interaction method compared to more recent calculations that provide (see Fig. 5) better agreement with experimental data on the radiative lifetimes of emission $c^1\Sigma_u^- \rightarrow a^1\Delta_g$; they also predict a higher probability of the co-operative transition 1–4. This gives grounds to hope that at a sufficiently high concentration of $O_2(a^1\Delta_g)$ in solution this transition can also be detected in absorption.

For the transition $b^1\Sigma_g^+ - a^1\Delta_g$ the component (4) is more active (transition 3–2) than the other quasi-degenerate component (4a) of the $a^1\Delta_g$ state (transition 3–1). This agrees with the results of the simplified analysis of relations (13) and (14) and with Fig. 3. The $b^1\Sigma_g^+ - a^1\Delta_g$ (3–2) transition is relatively intense at long R (3.8–4.2 Å), while at smaller R values the other, shorter-wavelength transitions are enhanced to a much greater extent (see Fig. 5). This is due to an increase in the contributions of charge transfer states to higher-energy terms.[109]

Curve *5* in Fig. 5 shows a rapid increase in the probability of the 4–5 transition as the molecules approach each other. This is a co-operative transition from the triplet state to the ground singlet state of ethylene with simultaneous excitation of the oxygen $c^1\Sigma_u^-$ state. At $R = 3$ Å, the dipole moment of this transition is 0.2 D, being commeasurable with the dipole moments of the allowed optical transitions.[13] For many dyes the wavelength of this co-operative transition falls in the visible region; observation of this transition in electric discharge may appear to be useful in studies of the concentration of the $c^1\Sigma_u^-$ states of the oxygen molecule and in the design of new chemical lasers.

The $S_0 - T_1$ transition of ethylene becomes an allowed triplet–triplet transition of the collision complex with oxygen (transition 0–6 in Fig. 2).[2, 12, 27, 70, 110] Formally, the dipole moment of the transition between the pure configurations, $X^3\Sigma_g^- \times S_0 - X^3\Sigma_g^- \times T_1$, equals to zero; however as configurational interaction causes the triplet states to mix and thus the contributions of charge transfer states and triplet states of the type $X^3\Sigma_g^- \times S_1$ appear, the 0–6 transition is collision induced.[70, 109] The $S_0 - T_1$ transitions of ethylene were observed upon adding oxygen at high pressure [111] and in many dye solutions.[2] The theoretical intensity [109] of the 0–6 transition matches experimental data;[111] this gives grounds to believe that calculations [109] are suitable for comparative predictions of the probabilities of some other triplet–triplet transitions including co-operative excitations. New intense transitions induced by oxygen–dye collisions were predicted.[12, 27, 109]

Of particular interest is the singlet–triplet transition 6–7 between two excited states, S_1 and T_1, of the dye. As the dye molecule contacts the triplet oxygen ($X^3\Sigma_g^-$), this transition not only becomes a dipole-allowed triplet–triplet transition, but also acquires the maximum intensity, which is due to comparatively large contribution of charge transfer states.[12, 70, 86, 99, 109] Indeed, the S_1 state of the dye has a relatively high energy (1.5–2 eV higher than that of the T_1 state) and stronger mixes with the charge transfer states. In the complex of O_2 with ethylene the dipole moment of the

$X\,^3\Sigma_g^- \times S_1 - X\,^3\Sigma_g^- \times T_1$ transition is 0.38 D at an intermolecular distance R of 3.6 Å which is similar to equilibrium one.[99] Commensurable, although smaller, values were obtained for the O_2 complexes with naphthalene and conventional dyes.[103] This 'colossal' enhancement of the $S_1 - T_1$ radiative transition, which is forbidden for free dye molecule, provides an explanation for the high rate of quenching of dye fluorescence.[27]

Analysis of calculations[99,109] also made it possible to explain the known enhancement of the Herzberg(III) band ($X\,^3\Sigma_g^- - A'\,^3\Delta_u$) at high pressure of oxygen or buffer gas and in inert gas matrices.[9,93,103] High intensity of the Herzberg(III) band and the $c^1\Sigma_u^- - a^1\Delta_g$ transition, as well as co-operative transitions involving the Herzberg state [104] is due to much more efficient mixing of π_u-MOs with the solvent orbitals rather than π_g-orbitals.[12] All features of the interaction between oxygen open shells and solvent molecules are clearly related to enhancement of radiative transitions. Taking account of this fact makes understandable numerous optical effects due to collisions between oxygen and organic dye molecules.[12,86]

5. Relation between enhancement of radiative transitions and quenching of dye fluorescence

The mechanism of enhancement of collision-induced radiative singlet–triplet transitions of oxygen is intimately related to the acceleration mechanism of non-radiative deactivation of $O_2(a^1\Delta_g)$ (Refs 26, 27, 81) and other quenching processes in the contact complex $O_2 + M$.[2,13,112–137] Within the framework of the model for dispersion forces the collision induced electric dipole moment of transition of the oxygen molecule can interact with the moments of transitions in solvent. Recall that the dipole–dipole interaction between all virtual transitions in two closely spaced molecules determines the attractive forces acting between them; this interaction is responsible for the dipole–dipole non-radiative energy transfer and (partially) for quenching of singlet oxygen.[1,2,27,71,115]

An explanation for various types of generation of singlet oxygen due to dipole-dipole energy transfer and CI-calculated transition moments in collision complexes is available.[27] Collision-induced dipole moments of S–T-transitions (forbidden in isolated molecules) are mainly due to exchange interaction; therefore, this type of energy transfer can be treated as exchange-resonant one.[107] However, in this case [27] its rate should be calculated using the expression for the dipole–dipole interaction between the moments of induced transitions. For instance, quenching of dye fluorescence can be explained by enhancement of non-radiative collision-induced $S_1 - T_1$-transition with $O_2(X\,^3\Sigma_g^-)$. Namely, a relatively large dipole moment of the $S_1 - T_1$-transition (D_{S-T}) induced by collisions between dye and oxygen molecules strongly interacts, by the dipole-dipole mechanism, with the moments of $T_{1,0} - T_{1,v}$ resonant transitions between vibrational sublevels of high-frequency C–H (O–H) vibrations and their overtones of the dye molecule.[2,27] This also makes understandable the contribution of charge transfer states to the quenching mechanism, because the D_{S-T} strongly depends on them.[27] Quenching of T_1 states through energy transfer to singlet oxygen depends on the intensity enhancement of the 0–6 and 1–3 (2–3) transitions and the $a-X$ transition; all of them become dipole-allowed transitions upon collision.[27] The applicability of the dipole–dipole mechanism is substantiated by the fact that the distance between the 'emitting' oscillator (induced dipole moment of the $S_1 - T_1$-transition) and 'absorbing' oscillators (overtones) is noticeably longer than the oscillator size, namely,[2] both 'dipoles' are at most 0.1 Å long.

The dipole moments of the $S_1 - T_1$-transitions in the O_2 complexes with ethylene [27] and naphthalene,[103] obtained from MINDO calculations with inclusion of configurational interaction are equal to 0.02 and 0.01 D, respectively, at an intermolecular distance of 3.2 Å. The D_{S-T} value rapidly increases as the molecules approach each other;[27,87] however, this is hard to reach in the gas phase under normal pressure. The vector of the dipole D_{S-T} connects the centres of the molecules, being distant from the C–H oscillators. The size and orientations of these oscillators are comparable with analogous parameters of H atom displacements.[2,86] Theory of non-radiative transitions in the case of non-adiabatic perturbation was considered in Ref. 2. Calculations of the rate of quenching of dye fluorescence by oxygen due to enhancement of non-radiative $S_1 - T_1$-transition give the rate constants of the order of 10^{13} litre mol^{-1} s^{-1}, which is much higher than the duffusion constants.[27]

6. Sensitisation of $O_2(a^1\Delta_g)$ molecule

Singlet oxygen is most often generated using photosensitisation, *i.e.*, energy transfer from excited state of sensitiser to $O_2(^3\Sigma_g^-)$ state. Possible sensitisers include many dyes absorbing visible light, in particular, widely abundant natural compounds, such as chlorophyll, haem, protoporphyrin and other porphin derivatives. Therefore, singlet oxygen plays an important role in many photobiological processes.

Excited singlet state of a dye sensitiser (S_1) formed upon absorption of a light quantum is efficiently quenched through oxygen-induced ISC [see Eqn (20)] or due to fast monomolecular transition to the T_1 state. Upon collision with $O_2(^3\Sigma_g^-)$, the long-lived state T_1 generates the quintet, triplet and singlet states of the collision complex. Decomposion of the singlet state into products is spin allowed

$$T_1 + {}^3O_2 \longrightarrow {}^{1,3,5}(T_1 + {}^3O_2) \longrightarrow \longrightarrow S_0 + {}^1O_2\,(a^1\Delta_g \text{ or } b^1\Sigma_g). \quad (23)$$

Quenching of phosphorescence of tripaflavin adsorbed on silica gel [reaction (23)], was proposed by Kautsky in 1931.[2,7] Experiments were carried out in a sealed vessel at low concentration of the oxygen added. Quenching was explained by the formation of active oxygen in the singlet state. According to Kautsky's hypothesis, $^1O_2$ reaches the oppositely lying surface of a silica gel bead containing adsorbed dye and transforms it to the coloured form. This hypothesis was soon forgotten and quenching of the T_1 states of organic molecules was explained by formation of unstable peroxide intermediates (moleoxides).[7] Only three decades ago Kautsky's ideas were completely substantiated.[1,2,7] Oxygen efficiently quenches the T_1 states of all organic molecules studied in vapours, liquid solutions, adsorbates and polymers (where diffusion of O_2 is possible).[1,2] The rate constant for quenching of triplets with oxygen ($k_T^{O_2}$) is about an order of magnitude lower than the rate constant for diffusion (k_d).

Since the quintet, triplet and singlet states of the collision complex are equiprobable, nine collisions on the average produce five quintets, three triplets and one singlet; only in the last-mentioned case reaction (23) is spin-allowed and only in this case singlet oxygen can be generated. Then one has $k_T^{O_2} \leqslant (1/9)k_d$, which is in agreement with many (not all) experimental data.[1,2] Complete quenching

$$T_1 + {}^3O_2 \longrightarrow S_0 + {}^3O_2$$

can start from the triplet state of the complex;[27] it also contributes to $k_T^{O_2}$. Quantum yield measurements confirmed the importance of this quenching channel.[131] Rate constant measurements for quenching of T_1 states of carotenoids gave $k_T^{O_2} \approx 10^9$ litre mol^{-1} s^{-1}. In this case the formation of $O_2(a^1\Delta_g)$ is impossible, because its energy exceeds that of the T_1-state,[1,131] which also points to important role of this channel of complete quenching.

IV. Quenching of the $O_2(a^1\Delta g)$ molecule

The main mechanism of quenching of singlet oxygen in the gas and liquid phases involves transfer of electronic excitation energy of the $O_2(a^1\Delta_g)$ to the vibrational degree of freedom of the collision partner.[2, 12, 26, 78, 116–122] In its pure form this mechanism occurs for quenchers with molecules having high oxidation potentials or high energies of triplet-excited states: here the mechanism of charge transfer [119] or quenching by transfer of electronic energy to triplet state is impossible.[1] The electronic excitation energy of the $O_2(a^1\Delta_g)$ is transformed to vibrational, rotational or kinetic energy of quencher. Noble gases are the poorest quenchers of singlet oxygen [1] (for argon, the second-order rate constant for quenching is $k_Q^\Delta = 5$ litre mol^{-1} s^{-1}) because in the gas phase their atoms have no vibrational degrees of freedom and cannot efficiently transform the electronic excitation energy of $O_2(a^1\Delta_g)$ to heat. However such gases as H_2 ($k_Q^\Delta = 2800$ litre mol^{-1} s^{-1}), NH_3 ($k_Q^\Delta = 2600$ litre mol^{-1} s^{-1}), C_6H_6 vapour ($k_Q^\Delta = 3200$ litre mol^{-1} s^{-1}) and water vapour ($k_Q^\Delta = 4900$ litre mol^{-1} s^{-1}) are the most efficient scavengers.[1, 118] All hydrides have high-frequency X–H bond vibrations (*e.g.*, $\omega_{sym} = 2916$ cm^{-1} for CH_4 molecule, $\omega_{asym} = 3939$ cm^{-1} for H_2O molecule, $\omega_e = 4401$ cm^{-1} for H_2 molecule);[2, 9] here two or three vibrational quanta are sufficient to absorb the energy of singlet oxygen (7918 cm^{-1}). Molecules containing no C–H or O–H bonds (*e.g.*, CS_2, CCl_4) are much poorer quenchers of singlet oxygen.[1, 78]

Initially, lifetime measurements of singlet oxygen in solutions were carried out by indirect chemical methods.[78, 120–122] By conducting steady-state photo-oxidation of benzofuran in solution with variable concentration of β-carotene, which physically quenches $O_2(a^1\Delta_g)$,[122] one can determine the product $\tau_\Delta k_Q^\Delta$. Assuming that the rate constant k_Q^Δ for β-carotene is diffusion controlled,[120] Young *et al.*[122] determined $\tau_\Delta = 5.5$ μs in methanol.[122] Later on,[77, 78, 121] direct lifetime measurements of singlet oxygen in solutions were carried out using pulsed lasers (a greater value was obtained in methanol, $\tau_\Delta = 9.5$ μs).[1, 106] Merkel and Kearns [78] were the first who noticed significant changes in τ_Δ for different solutions and applied the theory of transfer of the energy of oxygen $a^1\Delta_g$ electronic excitation to solvent vibrations. Later on, these results were repeatedly refined.[1, 73–77, 101–106, 116–118] According to recent data,[1, 102] the time τ_Δ varies from 3.1 μs (H_2O) to 128 ms (CCl_4) and 309 ms ($C_{10}F_{18}$), *i.e.*, within five orders of magnitude.

A number of quantitative theories of $O_2(a^1\Delta_g)$ quenching through transfer of electronic excitation energy to solvent vibrations were put forward.[1, 26, 78, 116, 118] (This energy transfer is called e–v-deactivation.[1, 76]) Merkel and Kearns [78] used the theory of dipole–dipole energy transfer and related τ_Δ to the optical density (OD) of IR absorption of the solvent at the 0–0 and 0–1 vibronic band wavelengths of the $a^1\Delta_g \rightarrow X^3\Sigma_g^-$ transition (1270 and 1592 nm, respectively)

$$\frac{1}{\tau_\Delta} = 0.5(OD_{1270}) + 0.05(OD_{1592}) + \quad (24)$$

$$+ \text{ higher-order corrections.}$$

Rodgers [117] measured τ_Δ for a number of solvents and determined the second-order rate constants for quenching of $O_2(a^1\Delta_g)$ by the solvent molecules A ($1/\tau_\Delta = k_{Q,A}^\Delta[A]$); then he measured the τ_Δ values in binary mixtures of solvents A and B and showed the validity of the following equation:

$$\frac{1}{\tau_\Delta} = k_{Q,A}^\Delta[A] + k_{Q,B}^\Delta[B]. \quad (25)$$

The study [117] not only appeared to be useful for practical purposes, but also confirmed that quenching of singlet oxygen in the liquid phase is also bimolecular in character. An important contribution of Hurst and Schuster [116] consists in thorough choice of solvents. A linear correlation between $1/\tau_\Delta$ and concentration of hydrogen per mole found for a series of aromatic compounds $C_6H_nF_{6-n}$ ($n = 1-5$) made it possible to introduce the second-order rate constants for quenching k_{CH}^Δ per C–H bond (irrespective of the number of fluorine atoms in the molecule). It follows that the quenching ability of the solvent is governed by a certain specific feature of C–H-bonds and that donor–acceptor interactions in these solutions are of no concern (since the fluorobenzenes studied possess the properties of donors). However, this does not mean that the interactions in question are insignificant for quenching of $O_2(a^1\Delta_g)$ in other media (*e.g.*, porphyrin solutions).

The dependences of $1/\tau_\Delta$ on the concentration of C–H bonds and on the OD-containing terms in expression (24) were compared.[116] It was found that the dependence on [CH] accounts more correctly for the solvent effect on the quenching rate and that the results of calculations using relation (24) are in poor agreement with experimental values of $1/\tau_\Delta$. Both parameters are interrelated (the higher [CH] the higher OD); however, the optical density of IR absorption explicitly depends on the dipole moment of the transition, so the results [116] cast some doubt on the dipole–dipole mechanism of energy transfer. Apparently, the exchange mechanism as well as the dipole–quadrupole one [26] also contribute to the quenching through e–v-deactivation.

Hurst and Schuster [116] proposed an expression for the second-order rate constant for quenching (k_{XY}^Δ) involving the X–Y bond in the solvent molecule

$$k_{XY}^\Delta = C_\Delta \sum_{mn} F_m F'_n R_{mn}. \quad (26)$$

Here C_Δ is the matrix element of electronic interaction, which includes the type-(11) term and is independent of the solvent; F_m and F'_n are the Franck–Condon factors for the $(0-m)$ vibronic band of the $a \rightarrow X$ transition and for the $(0-n)$ vibrational transition of the X–Y bond, respectively; and the factor R_{mn} characterises the resonance detuning between these two transitions. Table 3 lists a number of rate constants for quenching of singlet oxygen k_{XY}^Δ reported by Hurst and Schuster;[116] the data exhibit a large scatter.

Table 3. Second-order rate constants k_{XY}^Δ for quenching of $O_2(a^1\Delta_g)$ involving stretching vibrations of X–Y bonds in the solvent molecule.[116]

X–Y bond	Wave number /cm^{-1}	k_{XY}^Δ /litre mol^{-1} s^{-1}
O–H	3500	2000
O–D	2550	150
C–H	3050	420
C–D	2240	17

Schmidt and Brauer [118] studied solvents possessing poor quenching ability, the isotopomer $^{18}O_2$, and improved the Hurst and Schuster theory. For a large number of solvents the measured rate constants for quenching of singlet oxygen are reasonably well described by the relation [1, 116, 118]

$$k_Q^\Delta = \sum_{XY} N_{XY} k_{XY}^\Delta, \quad (26a)$$

where N_{XY} is the number of X–Y bonds in peripheric regions of the solvent molecule that are accessible to the interaction with molecular oxygen.

Quenching of singlet oxygen can be due to not only the dipole-dipole interaction, but also dipole – quadrupole interactions.[2, 26] The first estimation of the quadrupole moment of the $a-X$ transition showed [26] that it is stolen from the quadrupole moment of the spin-allowed $b^1\Sigma_g^+ - a^1\Delta_g$ transition. The stealing mechanism is identical to that described by relation (16) and is due to SOC-induced mixing of the X- and b-states (9) and (10). In addition, the dipole moment operator (D) in relation (16) should be replaced by the quadrupole moment operator (Q). The quadrupole moment of the $a-X$ transition is

$$Q_{a-X} = -cQ_{a-b} = 0.0038 \text{ e Å}^2.$$

It contributes negligibly to the radiating capacity[12] but largely to quenching of the $O_2(a^1\Delta_g)$ state through the dipole – quadrupole interaction.[26]

Collision-induced dipole moment of the $a-X$ transition of oxygen also interacts with the moments of weak overtone IR transitions of solvent and quenches the phosphorescence of O_2.[27] In both cases the rate constant for quenching should depend on the overlap of the emission spectra of singlet oxygen and IR absorption overtones of the solvent. Both predictions are in semiquantitative agreement with the results of indirect measurements τ_Δ.[2, 26, 78] However, direct (more accurate) measurements of $O_2(a^1\Delta_g)$ lifetime [116–118] did not confirm this correlation, probably, due to additional (undiscussed) contributions to the quenching mechanism.

As mentioned above, a unique spectral phenomenon, namely, observation of co-operative vibronic emission of singlet oxygen in solutions of halogenated hydrocarbons was explained.[28, 113] The $a-X$ wavelength experienced a bathochromic shift by the energy of the vibrational quantum of the solvent.[114] The dipole moment of the $a-X$-transition of oxygen in solution is induced by the collision of O_2 with the solvent molecule (M) and strongly depends on the intermolecular distance (R). Vibrations of the C–Cl bond in the molecule M upon collision of O_2 with the solvent molecule (see Fig. 4) strongly affect the R magnitude and give rise to the derivative of the dipole moment of the $a-X$ transition with respect to R. It is this derivative that determines the probability of co-operative vibronic emission of singlet oxygen accompanied by the bathochromic shift on the C–Cl vibrational frequency.[28, 113] The $a \rightarrow X$ transition of oxygen is accompanied by simultaneous excitation of C–Cl vibrations in the solvent molecule. Calculations of the derivative in Eqn (19) give a correct estimate of the intensity of this synchronised transition in the two molecules.[28, 113] The transition is two orders of magnitude less intense than the $a-X$ transition,[28] which agrees with experimental data.[114]

The theory [113] is important for not only understanding of weak co-operative emission,[114] but also explanation of deviations in the rate of $O_2(a^1\Delta_g)$ quenching from the values calculated using the simple theory of inductive-resonant energy transfer to solvent vibrations.[1, 2, 26, 60, 78] The rate of quenching of singlet oxygen is not always related to the overlap integral between the $a \rightarrow X$ emission spectrum and IR absorption spectrum of solvent overtones.[1, 60, 78] The frequency of the co-operative vibronic transition differs from the eigenfrequencies of oxygen appearing in Eqn (24), and the moment of this transition efficiently interacts with molecular vibrations of the solvent. In essence, the driving force of energy transfer is reduced to the coupling of the molecular vibrations of the solvent and the motion of electrons in the O_2 molecule with allowance for SOC [see Eqn (11)]. Electronic-vibrational interaction in the contact complex O_2 + M directly relates the electronic wave function of the $O_2(a^1\Delta_g)$ state to the intermolecular and internal vibrations in the molecule M. The intermolecular distance q in expression (19) determines not only the electronic-vibrational contribution to the dipole moment of the co-operative transition, but also the mixing with the molecular vibrations of the solvent. The intensity of the co-operative transition is very low; however, owing to direct character of energy exchange with the solvent vibrations it can contribute largely to quenching of singlet oxygen. Note that the results obtained using the simple theory of inductive-resonant energy transfer to solvent vibrations show the largest deviation from the experimental data for halogen-containing solvents.[26]

Yet another important mechanism of quenching of $O_2(a^1\Delta_g)$ is the inclusion of configuration interaction and SOC in the mixing with charge transfer states.[115] Unlike the universal mechanism of e – v-deactivation, the charge transfer mechanism manifests itself only for molecules with low oxidation potential ($\leqslant 1.9$ V *vs.* s.c.e.).[1] It is important to distinguish between this mechanism and actual charge transfer that occurs as the kinetic stage of quenching.[1, 115] We believe that this confusion [119, 121] often occurs in discussing the mechanism of quenching of $O_2(a^1\Delta_g)$. The dependence of the rate constant for quenching ($k_Q^\Delta = 1/\tau_\Delta$) on the ionisation potential (IP) of the quencher was found long ago.[119–122] Aliphatic amines do not react with $O_2(a^1\Delta_g)$, but efficiently inhibit the oxidation of other compounds possessing high reactivity towards singlet oxygen.[2, 119] Taking into account the increase in $\log k_Q^\Delta$ with a decrease in the amine IP, one can assume [119] that the charge transfer configurations (CTC) are mixed with the $a^1\Delta_g$ and $^3\Sigma_g^-$ states and somehow enhance the SOC between them. Explanation for this mechanism (also important for understanding of biochemical activation of oxygen) was reported.[115]

Now we will write the wave functions of the $a^1\Delta_g$ and $^3\Sigma_g^-$ states in a collision complex with amine molecule in the form [12, 115]

$$^3\Psi_0 = \left|S_0{}^3\Sigma_{g,0}^-\right\rangle = \frac{1}{\sqrt{2}}\left(\left|a\bar{a}\pi_x\bar{\pi}_y\right| - \left|a\bar{a}\pi_y\bar{\pi}_x\right|\right), \quad (27)$$

$$^1\Psi_1 = \left|S_0^1\Delta_g\right\rangle = \frac{1}{\sqrt{2}}\left(\left|a\bar{a}\pi_x\bar{\pi}_x\right| - \left|a\bar{a}\pi_y\bar{\pi}_y\right|\right). \quad (28)$$

Here a denotes the highest occupied molecular orbital (HOMO) of the aliphatic amine in the singlet ground state S_0, *i.e.*, the lone pair orbital of the nitrogen atom. Electrons of inner shells are left out of consideration. Note that the wave function (27) differs from that reported in Ref. 115 in permutation of two MOs and, hence, the sign of the determinant. Charge transfer from amine to the degenerate orbitals, $\pi_{g,x}$ and $\pi_{g,y}$, of the oxygen molecule gives four CTC, namely, two degenerate singlet and two triplet states in the radical pair $\{D^{+\bullet}O_2^{-\bullet}\}$ produced upon charge transfer (D denotes the electron donor).[115] We will consider only those configurations that are important for the explanation of the quenching mechanism,

$$^3\Psi_{ct_y} = \left|D^{+\bullet}O_2^{-\bullet}\right\rangle = \frac{1}{\sqrt{2}}\left(\left|\pi_y\bar{a}\pi_x\bar{\pi}_y\right| - \left|a\bar{\pi}_y\pi_y\bar{\pi}_x\right|\right), \quad (29)$$

$$^1\Psi_{ct_x} = \left|D^{+\bullet}O_2^{-\bullet}\right\rangle = \frac{1}{\sqrt{2}}\left(\left|a\bar{\pi}_x\pi_x\bar{\pi}_y\right| + \left|\pi_x\bar{a}\pi_y\bar{\pi}_x\right|\right). \quad (30)$$

Analysis of intermolecular interaction using the CI method revealed an effective mixing of the triplet configurations (27) and (29) in the collision complex. The singlet states (28) and (30) possess different symmetry with respect to reflection in the O–O–N plane, also being effectively mixed with each other due to CI. Mixing of the second singlet component (4a) with the CTC (30) is impossible. The inclusion of intermolecular interaction in the framework of the CI method gives the $^3\Psi_0 + \varepsilon^3\Psi_{ct_y}$ and $^1\Psi_1 + \delta^1\Psi_{ct_x}$ states which strongly interact

with each other due to SOC.[115] The matrix element of the SOC operator between these states includes the integral

$$\varepsilon\delta^* \left\langle {}^3\Psi_{\mathrm{ct}_y} \middle| H_{\mathrm{so}} \middle| {}^1\Psi_{\mathrm{ct}_x} \right\rangle = \frac{\varepsilon\delta^*}{2} \langle \pi_y | B_z | \pi_x \rangle = \frac{\varepsilon\delta^* \mathrm{i}}{2} \zeta_{\mathrm{O}}\,, \qquad (31)$$

where ε and δ are the admixture coefficients to the $a^1\Delta_g$ and $X^3\Sigma_g^-$ states, respectively.

Relations (27), (29) and (31) include the wave functions of the triplet states with the zero projection of the total spin on the z axis. Comparison with expression (8) shows that the SOC between the CTC (29) and (30) is reduced to the same integral between the degenerate orbitals, $\pi_{g,x}$ and $\pi_{g,y}$, of the oxygen molecule, as that appearing in the matrix element of the SOC between the states (5). Thus, the presence of CTC admixtures always gives rise to the SOC between the $a^1\Delta_g$ and $X^3\Sigma_g^-$ states, which accelerates the non-radiative transition and quenching of singlet oxygen.[115] The admixture coefficients ε and δ to the states become significant only for the quencher molecules having low oxidation potentials ($\leqslant$1.9 V *vs.* s.c.e.). Otherwise, the CTC energy is too high while the CTC admixture coefficients in Eqn (31) are negligible. According to calculations,[12, 27, 34, 70, 99, 103] for molecules with ionisation potentials higher than 10.5 eV the ε and δ values are at most 0.01, the integrals (31) being negligible.

Charge transfer configurations (29) and (30) differ in spin and population of the $\pi_{g,x}$ and $\pi_{g,y}$ orbitals. The matrix element of the SOC operator between them can be treated as an electron 'jump' from the $\pi_{g,y}$-MO to the $\pi_{g,x}$-orbital with a spin flip. This 'jump' is identical to rotation of the orbital, *i.e.*, the appearance of an orbital angular momentum or ring current, which induces the magnetic moment interacting with the spin. Since the case in point is the quantum singlet – triplet transition, visual interpretation of this effect is, strictly speaking, inadmissible.[15] However, the simplified ideas of an electron 'jump' and orbital rotation are useful in revealing the essence of the mechanism of quenching of singlet oxygen by amines due to admixtures of charge transfer states.

Strengthening of the SOC (to some extent) between the $a^1\Delta_g$ and $^3\Sigma_g^-$ states of the O_2 molecule due to CTC contributions always occurs in collision complexes. It is determined by the weight factors of the admixtures ε and δ, which are large only for donor lone electron pairs with low ionisation potential provided a local character of donor – acceptor interaction.[115] At present, exact determination of the contributions of different mechanisms to the rate constant for quenching k_Q^{Δ} is impossible owing to the difficulties in the inclusion of vibrational modes of the solvent molecules in the nearest environment of the $O_2(a^1\Delta_g)$ molecule. The concept of admixtures of the charge transfer states [see Eqns (29) – (31)] is fundamentally important for analysis of the mechanisms of biochemical activation of oxygen by oxidases.

V. Biochemical activation of the molecular oxygen

Nearly 100 years ago Academician A N Bach first studied breath from the standpoint of oxygen activation.[137 – 139] Based on the concepts of classical chemistry, he assumed the necessity of cleaving a bond in divalent oxygen and release of a chemical valence for addition of other compounds. According to Bach, the corresponding activation energy should be supplied from readily oxidisable unsaturated compounds; O_2 adds to them to give peroxides that degrade under the action of enzymes, and oxygen is transferred to other substrates that are incapable of immediately adding to atmospheric oxygen.[137] Clearly, at that time it was impossible to allow for specific quantum features of microparticles constituting the molecule, in particular, the spin. The energy of spin-related magnetic interactions is low, however it should be taken into account when studing not only line splitting in atomic optical spectra and in EPR spectra of radicals,[13, 38, 46 – 49, 84, 138, 139] but also the mechanisms of certain chemical reactions.[12, 37, 140 – 149] In spite of rapid progress in biochemistry and detailed knowledge of molecular mechanisms of the action of many enzymes, the nature of bioactivation of oxygen is still unclear.[5, 6, 150, 151] Below we will show that it is the magnetic and exchange spin effects that are often responsible for activation of molecular oxygen by oxidase co-enzymes. The nature of these effects has much in common with the mechanisms considered above when we analysed the photophysical properties of oxygen.

1. Role of spin in chemical reactions involving oxygen

Two unpaired electrons in antibonding π_g-MOs are responsible for specific character of the interaction of molecular oxygen with radicals (combustion) and chemically stable diamagnetic compounds (slow oxidation). Two antibonding π_g-vacancies make it possible to transform O_2 to O_2^- and O_2^{2-} anions, the formation of the latter being strongly dependent on the presence of electron donors (enzymes) and magnetic perturbations that affect the spin prohibitions.

In 1937, Pauling established that the magnetic moments of hemoproteins decrease as the pH values of solutions increase. The effect was explained by the iron ion spin flip owing to small changes in the coordination of ligands.[5] The total spin of the Fe^{3+} ion is determined by the number of unpaired electrons in the 3d-shell of the metal. The low-spin state ($S = 3/2$) becomes more stable than the state with $S = 5/2$ as the pH value increases; the transition between these states is induced by the spin – orbit coupling in the 3d-shell of the metal. In weak ligand field the unfilled 3d-shell has degenerate orbitals and the states with different spins have similar energies. Recall that the spin quantum number of one electron ($S = 1/2$) determines the absolute value of the momentum vector

$$\sqrt{\vec{S}^2} = \sqrt{S(S+1)}\hbar = \frac{\sqrt{3}}{2}\hbar.$$

The summation of electron spins obeys the quantum addition rules,[15] so the total spin of the molecule is zero at 'antiparallel spins (all spins are paired); such state is called a singlet state. Most chemically stable organic compounds and corresponding oxidation products are diamagnetic, *i.e.*, they have no intrinsic magnetic moment (all spins are paired due to saturation of valences; the total spin of the molecule $S = 0$). Spins can undergo 'depairing' when exposed to light; here an electron goes to a vacant MO; according to the Pauli principle, both spins can be parallel (total spin $S = 1$). This excited state is called a triplet state because of three possible orientations of the total spin vector $M_S = \pm\hbar, 0$.

Singlet – triplet transitions are spin-forbidden;[15] this is a strict prohibition, because it can be removed only in the presence of magnetic interactions that are much weaker than electric ones.[13] The latter determine the energies of chemical bonds and excited states and the pathways of chemical reactions. The spin affects the energy through exchange interaction.[15] A weak SOC slightly mixes the singlet and triplet states of molecules, which gives a nonzero rate of S – T transitions that are observed in the form of phosphorescence and are well known in photochemistry.[2, 7, 13] Non-radiative S – T transitions also play an important role in the dark reactions, in particular, in catalysis.[12, 32] Weak SOC acts as a 'key' needed to open a 'heavy door', that is, the system chooses a pathway of chemical reaction with low activation barrier in the triplet state instead of overcoming a high activation barrier in the singlet state. Recall that the exchange integral appears with different signs in the energies of the S and T states, namely, two radicals form a chemical bond in the S state and repel in the T-state.[15]

Unlike most chemically stable organic compounds the O_2 molecule has the triplet ground state. According to Hund's rule, two unpaired electrons in two degenerate $\pi_{g,x}$ and $\pi_{g,y}$ orbitals (configurations π_g^2) have a lower repulsive energy in the triplet state [see Eqn (5b)] compared to the singlet state [see Eqn (5a)]. Because of this oxygen is paramagnetic (it has intrinsic magnetic moment due to spins of two unpaired electrons) and its addition to organic compounds is spin forbidden: starting reactants have the total spin $S = 1$, whereas the oxidation products are diamagnetic ($S = 0$).[6] Because of spin prohibition, combustion of organic fuels requires activation in the form of high-temperature ignition stage, *i.e.*, generation of primary radicals.[6–8] Reaction of $R^{\bullet}$ radical (one unpaired electron, $S = 1/2$, doublet state) with O_2 molecule is spin-allowed, because the starting reactants ($O_2 + R^{\bullet}$) and product ($RO_2^{\bullet}$) have doublet states, which provides the chain character of radical reactions

$$\underset{O_2}{[[\uparrow][\uparrow]]} + \underset{R^{\bullet}}{[\downarrow]} \Rightarrow \underset{RO_2^{\bullet}}{[[\uparrow\downarrow][\uparrow]]}, \qquad (32)$$

Here the quantum cell denotes the MO (see above).

Radical $RO_2^{\bullet}$ can decompose into radicals $RO^{\bullet}$ and $^{\bullet}O^{\bullet}$, thus making chain branching possible. In radical chain oxidation (combustion) processes the energy is released uncontrollably in the form of heat and light.[8] Clearly, this mechanism of oxidation with molecular oxygen cannot take place in living cells. However, cells meet their energy needs in the course of metabolic processes using the energy of oxidation of organic compounds under the action of oxygen.[5] Since cells cannot resist large temperature gradients, they should transform the energy released through oxidation to some kind of chemical energy prior to dissipation in the form of heat. This occurs by combining oxidation with the synthesis of adenosine triphosphate (ATP).[5, 139] In turn, the cell uses the ATP energy to carry out all endogenic processes, such as chemical syntheses of DNA and proteins, ion transport and mechanical work.[139] All versatile energy-supplying metabolic processes and reactions occur under subtle enzymatic regulation.[5] Is it spin-dependent? Despite the fact that to date many reactions of enzymes and metabolic pathways have been studied in detail,[143–147] the role of spin in biological oxidation of molecular oxygen is still unclear.[148–158]

2. Cytochrome oxidase

The simplest type of oxygen activation by enzymes containing metal cations involves the formation of intermediate peroxide ions O_2^{2-}. Reduction of O_2 by direct insertion of an electron pair into the filled π_g-orbitals requires spin changes, because the π_g^4 configuration can only be a singlet. Intermediates containing O_2^{2-} are formed in, *e.g.*, cytochromes.[5, 139] The $Fe^{3+}-O^{-}-O^{-}-Cu^{2+}$ structure, where the peroxide group is formed from the triplet oxygen and stabilised at its position until introduction of the second electron pair, is quite possible intermediate.[143] Apparently, electron transfer and formation of O_2^{2-} involves a triplet–singlet quantum transition called spin inversion.[145, 148] Cytochrome oxidase catalyses four-electron reduction of oxygen molecule to water. No intermediates were detected in the reaction

$$O_2 + 4\,e + 4\,H^+ = 2\,H_2O.$$

However, experimental measurements [5, 158] proved the formation of O_2^{2-}. The reaction centre of cytochrome oxidase includes one haem iron atom and one copper atom. The oxygen molecule binds to the haem Fe^{2+} cation and to Cu^+ ion that donate one electron each to form an O_2^{2-} anion. This provides a way to overcome the major obstacle to oxygen activation, that is, spin inversion (T–S transition).[145] Since the O_2^{2-} dianion has a filled electron shell, the ground state of this species is totally symmetrical and characterised by the term $|^1\Sigma_g^+\rangle$. Transfer of two electrons causes the ground-state term, $|X\,^3\Sigma_g^-\rangle$, of the O_2 molecule to smoothly transform to the term $|^1\Sigma_g^+\rangle$ of the dianion. The spin–orbit coupling between the states $|^3\Sigma_g^-\rangle$ and $|^1\Sigma_g^+\rangle$ is symmetry-allowed [see Eqn (8)]; therefore, the reduction

$$O_2(X\,^3\Sigma_g^-) \longrightarrow O_2^{2-}(^1\Sigma_g^+)$$

is also symmetry allowed with inclusion of the SOC. Since the SOC integral [see Eqns (8) and (11)] reaches its maximum value owing to symmetry of the oxygen MOs, one can expect that reduction of the oxygen molecule to the dianion should be accelerated due to effective removal of spin prohibition. These qualitative considerations should be complemented by analysis of the structure of the 3d-shells of the metal ions.[148]

Transition of the active site of cytochrome oxidase to the singlet state removes spin prohibition to subsequent fast chemical reactions up to formation of stable diamagnetic products.[5] According to calculations, the spin–orbit coupling that induces the T–S transition involves not only oxygen π_g-MOs, but also electronic changes in the 3d-shell of the iron ion.[133, 148]

The SOC mechanism can be represented as follows.[145, 148] Activation upon electron transfer to O_2 first involves excitation of Fe^{2+} ion (3d → 4s) to form the $^{1,3}D$ terms. Combination of two triplet states (iron and oxygen) gives the singlet, triplet and quintet states similarly to the case for collision of triplet oxygen and ethylene molecules (states 4 and 6, see Fig. 2). A singlet combination of two triplet states in the initial structure of cytochrome-*c* oxidase is shown in Scheme 1. The T–S transition in this quasi-degenerate pair is formed in the electron shell of the iron ion. The SOC is relatively weak and spin inversion is a relatively slow process. This is the reason for much lower (compared to the expected [5]) reactivity of O_2 towards certain ligands present in cytochromes. The singlet state formed upon T–S transition is shown on the left side of Scheme 1. Transition from this state to the peroxide form O_2^{2-} owing to transfer of two electrons from the metal ions is now spin allowed. This and subsequent processes occur in the singlet states.

Scheme 1

$[\uparrow][\uparrow].....[\downarrow][\downarrow].....[\uparrow\downarrow]$	$[\uparrow][\ ].....[\uparrow\downarrow][\downarrow\uparrow].....[\downarrow]$
3d 4s $\pi_{g,x}\,\pi_{g,y}$ 3d	3d 4s $\pi_{g,x}\,\pi_{g,y}$ 3d
Fe(II).....O_2.....Cu(I)	Fe(III)..... O_2^{2-} ..... Cu(II)

This mechanism of spin inversion occurs in hemerythrin and hemocyanin.[144] Cytochromes containing different protein residues coordinated to the iron ion can include Fe(II) ions in different spin states. Particular cytochromes have iron ions in the triplet ground spin state.[144] In this case reduction of the oxygen molecule to the dianion should occur in accordance with Scheme 1 (see above) with a very high probability without involving SOC.

3. Flavoproteins

Usually,[5, 139, 148–153] it is assumed that one can overcome the spin prohibition to oxidation of organic substrates with atmospheric oxygen by successive addition of single electrons in the reduction of O_2

$$O_2 + e \longrightarrow O_2^{-\bullet}, \qquad (33)$$

$$O_2^{-\bullet} + H^+ \longrightarrow HO_2^{\bullet}, \qquad (34)$$

$$HO_2^{\bullet} + H^+ + e \longrightarrow H_2O_2. \qquad (35)$$

Further reactions of diamagnetic hydrogen peroxide are spin allowed. It is assumed [5] that removal of spin prohibition in

reactions (33)–(35) proceeds as in the case of radical-chain oxidation where the spin prohibition can be removed upon formation of primary radicals. The author of this review found no clear discussion of the issie in biochemical literature (see, *e.g.*, Refs 5, 6, 152 and 153). A fundamental difference between the enzymatic reactions (33)–(35) involving radicals and the radical reactions of the type (32) in chain oxidation processes should be emphasised. In the latter case radicals go to the bulk of gas plasma flame (or in the solution bulk) and do not longer retain the 'spin memory' about precursors. All participants of biochemical oxidation reactions (33) and (35), *i.e.*, oxygen and electron transfer agents, are confined within the same active site of enzyme. If an electron is transferred to the oxygen molecule from diamagnetic enzyme, reaction (33) produces a radical ion pair [see Eqn (29)], all spins remain correlated, the 'spin memory' is retained and the spin prohibition to subsequent reactions (34) and (35) of a radical ion pair (triplet precursor) thus generated remains valid.

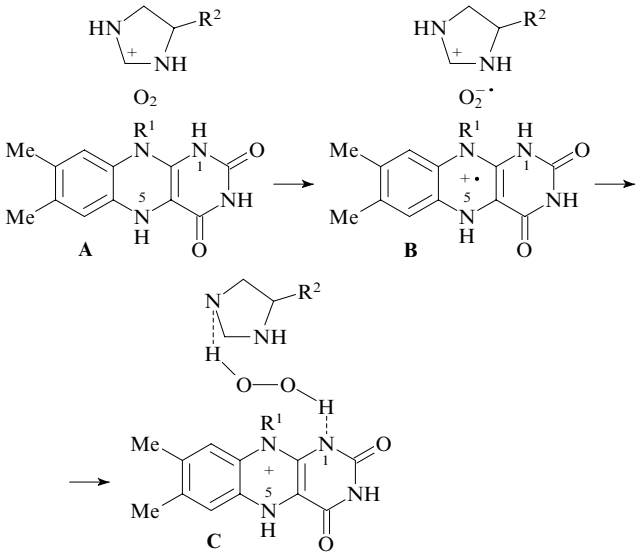
Many researchers believe that the oxygen molecule is very stable and can hardly add one more electron to give a radical anion $O_2^{-\bullet}$; as a consequence, they emphasise that stage (33) is the limiting one.[5, 139] Further addition of electrons is facilitated and subsequent reduction occurs readily.[5, 139] The bottleneck of this commonly accepted scheme is that the difficulty of electron addition to O_2 contradicts experimental data, namely, the process is exothermic and occurs with energy release (42 kJ mol^{-1}, see Refs 9 and 55). Enzyme molecules are designed in such a fashion that electron transfer in the respiratory chain be easy.[5] Indeed, reduced flavoproteins have very low ionisation potentials and are readily oxidisable.[139] If an O_2 molecule is delivered to the active site of an oxidase and interacts with flavoprotein, there are no physical prerequisites to assume that electron transfer to the oxygen molecule should proceed with difficulty.[149] The obstacle consists in the need of spin flip in the electron transfer stage (33) and formation of a triplet radical ion pair rather than addition of an electron to O_2.

To clarify the situation, we will consider glucose oxidase as an example.[3, 37, 148] Reaction (33) in glucose oxidase involves flavine adenine dinucleotide (FAD). Such compounds (flavoproteins) are typical of many co-enzymes; they were discovered in 1932 ('yellow enzyme' capable of catalysing the oxidation of nicotinamide nucleotides was isolated from yeasts).[5] Flavoproteins transfer electrons, as constituents of hydrogen atoms, from organic substrate to the riboflavin component of the enzyme using nicotinamide adenine dinucleotide (NAD^+) and its reduced form (NADH).[5, 139] The structures of these molecules were undoubtedly 'selected' by Nature to impart corresponding redox potentials to the co-enzymes.[150] NAD^+ exists in individual form and diffusionally moves from one enzyme to another, whereas FAD is tightly bound to protein. Flavoproteides tend to attach H atoms from one substrate and then transfer them to the other (O_2), being added to the same enzyme.[5] A covalent or hydrogen bond connects FAD to the residue of the polypeptide protein chain; therefore, FAD remains bound to a particular amino acid after proteolysis.

The action of glucose oxidase involves two stages, namely,[5, 155] glucose oxidation to gluconolactone with reduction of FAD to $FADH_2$ and the reverse cycle, $FADH_2 \rightarrow$ FAD, with reduction of O_2 to H_2O_2. From the standpoint of oxygen activation it is of interest to consider the second stage.

The active site of glucose oxidase from *Aspergillus Niger* has a histidine residue (His516) near the flavin ring of FAD; the distance between the protonated nitrogen atom N^{ε} of histidine and the N(1) atom of $FADH_2$ is about 4 Å (see Ref. 152). Scheme 2 presents a model for the active site of glucose oxidase. The first phase of the catalytic cycle involves reduction of FAD to $FADH_2$. The initial model **A** illustrates the O_2 insertion into the active site between the histidine residue of the protein chain and the N(1) atom; model **B** illustrates transfer of an electron from $FADH_2$ and formation of a radical pair; and **C** is the second to the last phase of the catalytic cycle accompanied by the formation of hydrogen peroxide. The last-mentioned stage involves abstraction of a proton from the N(5) atom and its transfer to histidine across the system of H-bonds in the protein and aqueous environments.

Scheme 2



When entering the active site, the O_2 molecule occupies the cavity between these atoms and then transfer of an electron from $FADH_2$ to the oxygen molecule occurs.[148]

$$FADH_2 + O_2 \longrightarrow FADH_2^{+\bullet} + O_2^{-\bullet}. \qquad (36)$$

This results in the formation of a triplet radical pair $\{FADH_2^{+\bullet} \cdots O_2^{-\bullet}\}$ in the active site of glucose oxidase, because the precursor of O_2 is in the triplet state, whereas that of $FADH_2$ is in the singlet state. According to density functional calculations (B3LYP/6-31G*),[3] electron transfer is almost thermally neutral (thermal effect of reaction is 0.6 kJ mol^{-1}).

In glucose oxidase, the O_2 molecule is transformed to superoxide ion $O_2^{-\bullet}$ upon addition of an electron, thus being activated.[3, 148] This slow stage is followed by fast proton transfer from the protonated histidine residue and simultaneous transfer of hydrogen atom from semi-oxidised radical $FADH_2^{+\bullet}$, which results in the formation of hydrogen peroxide.[148, 150]

4. Electron transfer in glucose oxidase and the spin flip

Now we will return to the key issue, namely, why the electron transfer stage (36) is slow ($k < 10^{-3}$ s^{-1}). According to calculations, electron transfer to the active site of glucose oxidase should occur spontaneously and rapidly ($k = 10^{-9}$ s^{-1}), just as O_2 will enter the active site. The O_2 molecule is characterised by a positive electron affinity (0.45 eV), *i.e.*, the addition of an electron is energetically favourable.[9, 44, 55, 154] Reduced FAD readily donates an electron; indeed, $FADH_2$ has a relatively low ionisation potential.[3] The reason is clear. The lowest occupied MO (LUMO) of the FAD molecule is the π^*-orbital of the isoalloxazine ring. In spite of the non-planar structure of this nucleus in $FADH_2$, its highest occupied molecular orbital is similar to the LUMO of the FAD molecule. Both orbitals are mainly localised on the central ring of the flavin nucleus.[150] This confirms a simple MO pattern obtained in the Hückel calculations, namely, the FAD LUMO is identical to the $FADH_2$ HOMO. Namely, the addition of two hydrogen atoms to the N(1) and N(5) atoms

is similar to attachment of two π-electrons to the ring π-system. From this a considerable decrease in the ionisation potential on going from FAD to $FADH_2$ becomes clear. The electron affinity of the O_2 molecule is much lower than the ionisation potential of $FADH_2$; however, when O_2 contacts protonated histidine, electron transfer becomes energetically favourable. Electrostatic attraction between the histidine cation and newly formed superoxide $O_2^{-\bullet}$ is the primary driving force of electron transfer and reduction of corresponding activation energy. It also facilitates strengthening of the SOC.

Thus, the active site of glucose oxidase is 'tuned for oxygen activation through electron transfer followed by spin flip according to Scheme 3.

Scheme 3

$$\underset{\text{Triplet}}{[\uparrow\downarrow].....[\uparrow][\uparrow]\ FADH_2\cdots O_2} \xrightarrow{ET} \underset{\text{Triplet}}{[\uparrow].....[\downarrow\uparrow][\uparrow]\ FADH_2^{+\bullet}\cdots O_2^{-\bullet}} \xrightarrow{SOC} \underset{\text{Singlet}}{[\uparrow].....[\downarrow][\uparrow\downarrow]\ FADH_2^{+\bullet}\cdots O_2^{-\bullet}}$$

TE is transfer of an electron.[145]

Simultaneous occurrence of reactions (34) and (35) resulting in diamagnetic products requires flip of one spin in the radical pair stage, *i.e.*, a triplet–singlet quantum transition. Such a transition is induced by the spin–orbit coupling, *i.e.*, magnetic interactions due to the orbital and spin motions of electrons (see Scheme 3).[3]

Spin flip is actually due to relatively strong SOC characteristic of radical pairs including superoxide ions.[3] In Scheme 3 the quantum cells denote the HOMOs of both molecules, that is, $FADH_2$ and O_2. As in the case of quenching of singlet oxygen by amines, where the role of CTC was shown [see Eqns (29), (30)], Scheme 3 presents different orbital structures of the triplet and singlet CTC. The starting triplet radical pair corresponds to a CTC described by Eqn (29), that is, transfer of an electron to the $\pi_{g,y}$-MO of O_2 molecule, whereas the singlet radical pair corresponds to a CTC described by Eqn (30), namely, transfer of an electron to another degenerate orbital of oxygen, $\pi_{g,x}$. The SOC arises between these CTC and is maximum possible for a system comprised of light (oxygen, nitrogen and carbon) atoms.

Actually, the formation of superoxide is not difficult. Indeed, a triplet radical pair is easily formed just after transfer of H atoms and reduction of FAD to $FADH_2$. The problem is to carry out a triplet–singlet transition in the radical pair $\{FADH_2^{+\bullet}\cdots O_2^{-\bullet}\}$ generated in reaction (36), because only the singlet pair can produce peroxide: reactions (34) and (35) involving protonated histidine and radical $FADH_2^{+\bullet}$ proceed concertedly.[3, 148] Reaction (34) has no effect on electron spins and in reaction (35) the spins remain correlated as in the initial state. Therefore, the initial steps of chemical reactions (34) and (35) should involve a spin flip (T–S transition from the triplet radical pair created upon electron transfer). In accordance with Scheme 3 the SOC integral includes the same components as the integrals (8) and (31)[3, 37, 148]

$$\langle {}^3\Psi_{ct_y}|H_{so}^Z|{}^1\Psi_{ct_x}\rangle = \langle \pi_y|B_z|\pi_x\rangle = \frac{i}{2}\zeta_O = 76.5\,i\ cm^{-1}. \quad (37)$$

The absolute value of this integral equals half the splitting between the ground-state terms $\Omega = 1/2$ and $\Omega = 3/2$ of the superoxide ion $X\,^2\Pi_g$ (*cf.* experimental value of 160 cm^{-1} (Ref. 9), which is in good agreement with our estimate [154]). The rate constant for the triplet–singlet transition can be estimated using the Fermi golden rule [13]

$$k_{T-S} = \frac{2\pi\rho}{\hbar}|\langle {}^3\Psi_{ct_y}\left|H_{so}^Z\right|{}^1\Psi_{ct_x}\rangle|^2 FC, \quad (38)$$

where FC is the Franck–Condon factor and ρ is the density of final states.

The SOC integral (37) is relatively large; usually,[12, 13] the matrix elements of the SOC operator for the molecules comprised of the first or second row elements are of the order of 1–10 cm^{-1}. These SOC integrals provide the rate constants for triplet–singlet transitions that are 10^6–10^4 times lower than the rate constants for spin-allowed transitions.[13] The SOC integral (37) provides the rate constant k_{T-S} that can be compared with the rates of other chemical reactions that are, in principle, possible during existence of the triplet radical pair $\{FADH_2^{+\bullet}\cdots O_2^{-\bullet}\}$ (back electron transfer, decomposition to new radicals). Despite the fact that the T → S transition in the $\{FADH_2^{+\bullet}\cdots O_2^{-\bullet}\}$ pair is relatively slow, it is much more efficient than typical T → S transitions in organic molecules and undoubtedly occurs in the active site of glucose oxidase. Subsequent reactions (34) and (35) in the singlet state of the entire flavoprotein system have low activation energies [3] and proceed rapidly. Transfer of a proton from the N^{ε} atom of the histidine fragment [see reaction (34)] is accompanied by proton transfer from the N(1) atom of $FADH_2$ to give hydrogen peroxide [see reaction (35)] with an the activation energy of only 29 kJ mol^{-1} (see Ref. 3).

Since the SOC integral (37) is only determined by the specific character of O_2^- anion and does not depend on the co-enzyme cation (K), effective T–S transitions in radical pairs $\{K^{+\bullet}\cdots O_2^{-\bullet}\}$ should occur in the activation of oxygen by flavoproteins and other oxidases following reactions (33)–(35). This mechanism of the T–S-transition in the radical pair is similar to spin relaxation in the superoxide ion.[145, 148]

5. Other examples of biochemical activation of oxygen

An important mechanism of enzymatic spin catalysis is characteristic of oxidases containing paramagnetic metal ions.[37, 145, 149, 156–158] Let us consider the exchange mechanism of acceleration of T → S transitions in radical pairs $\{K^{+\bullet}\cdots O_2^{-\bullet}\}$ taking copper amine oxidase as an example. This enzyme contains a bound quinonoid cofactor (topaquinone) near the Cu(II) ion coordinated to the ligands.[149] Consider the limiting stage of the operation of this enzyme, which can also be represented by the common processes (33)–(35). A radical pair $\{K^{+\bullet}\cdots O_2^{-\bullet}\}$ in the T-state is formed in the reaction of the type (36). The T → S transition is activated by exchange interactions with the copper ion following the scheme

$$K^+(\uparrow) + O_2^-(\uparrow) + Cu(II)(\downarrow) \longrightarrow K^+(\uparrow) + O_2^-(\downarrow) + Cu(II)(\uparrow). \quad (39)$$

Exchange interaction with copper ion for the superoxide ion is much stronger than for the co-enzyme (K^+) radical cation; therefore, the T → S transition of the radical pair is rather fast.[37] Measurements of kinetic isotope effects showed that replacement of the ^{16}O isotope by ^{18}O significantly slows down the limiting stage of oxygen reduction to peroxide for all enzymes studied.[152] In this case the Franck–Condon factor decreases; therefore, the proposed scheme of enzymatic spin-catalysis [3, 37, 148–150] provides a complete explanation for all results obtained in the kinetic studies on molecular oxygen activation by the enzymes mentioned above.[3, 152]

We will complete our comparative analysis of oxygen activation mechanisms taking cytochrome oxidase as an example; this compound catalyses four-electron reduction of O_2 to water in the final reactions of aerobic metabolism.[5] This is a very important process in the chain of continuous redox reactions involving proton transfer across membranes and creation of chemiosmotic gradient for ATP synthesis.[139, 157]

Cleavage of the O–O bond in cytochrome oxidase is a related to transfer of electrons and protons across mytochondrial membranes and to the formation of Fe(IV)=O groups in

a complex manner.[158] Note that the O—O bond dissociation, which continuously occurs in upper atmosphere, produces two highly reactive biradicals $O(^3P) + O(^3P)$ having four unpaired electron spins. (The process is spin allowed and can occur in the dark.) These species possess extremely high reactivity, but at low gas concentration the reactivity 'dissipates' into recombination, atmospheric emission and particularly, ozone synthesis. The O—O bond dissociation in cytochrome oxidase also causes 'depairing' of four spins and could produce two biradicals. Would these biradicals escape from the active site of enzyme to the bulk of proteins, they would 'burn out' mytochondria and cytoplasm. It is of great importance to cleave the O—O bond in cytochrome oxidase using the concerted mechanism consistent with other reactions, and thus chemically bind oxygen atoms and simultaneously 'quench' the spin. As shown above, in such enzymes chemical reactions are governed by the SOC and weak exchange interactions involving spins of paramagnetic iron and copper ions.[5] Spin catalysis favours fast and efficient (with small energy expenditure) dissociation of the O—O bond in the oxygen molecule.

Quantum chemistry is a unique tool for understanding of vitally important processes.[156–160] Similarly to quantum mechanics, which provides explanation for very subtle effects of spin interaction in solids,[161–164] quantum chemistry makes it possible to study electron-spin dependent properties of living matter.

VI. Conclusion

Removal of spin prohibition on singlet–triplet transitions in oxygen molecule interacting with buffer gas, solvent or coenzyme molecules in complex biopolymers is in some cases determined by certain common mechanisms. Physical substantiation of the mechanisms of bio-activation of oxygen is impossible if simpler mechanisms of O_2 photo-activation in solutions of organic dyes or upon collisions with other molecules in the gas phase remain unclear. In this review the term 'photo-activation' means acceleration of radiative and nonradiative triplet–singlet transitions in oxygen molecule induced by collisions with the solvent molecule, including sensitisation of singlet oxygen.

Analysis of the mechanisms of $O_2(a^1\Delta_g)$ quenching is closely related to these problems, being very important for understanding of the mechanism of bio-activation of oxygen. We considered the electronic structures and energies of various low-lying states of the O_2 molecule and the collision complexes of oxygen with simple (H_2, N_2, CH_3Cl, C_2H_4) and more complex molecules (benzene, naphthalene, dyes). The inclusion of specific spin–orbit coupling in the open π_g-shell of oxygen makes it possible to explain the intensities of the T—S transitions of the O_2 molecule and collision complexes. Selective enhancement of the intensity of the $a^1\Delta_g \rightarrow X^3\Sigma_g^-$ radiative transition upon collisions and its quenching in various solvents (M) was explained. The contribution of $M^+ - O_2^-$ charge transfer causes the SOC between the T—S states of oxygen to strengthen, which enhances the quenching of $O_2(a^1\Delta_g)$. Enzymatic activation of oxygen by, *e.g.*, glucose oxidase proceeds by a similar mechanism of T—S-transitions.

The mechanisms of activation and quenching of singlet oxygen involve energy transfer, which depends on exchange interactions, SOC, charge transfer, intra- and intermolecular vibrations. Based on analysis of the physical mechanisms of photo-activation, three types of oxygen activation by oxidase enzymes were proposed. They involve intermediate formation of the superoxide ion, O_2^-, and peroxide ion, O_2^{2-}. Elucidation of O_2 activation mechanisms due to T—S transitions in oxygen-binding enzymatic complexes opens new fields of investigations in biotechnology, namely, research on magnetic biopolymers and the effect of magnetic and microwave fields on the rate of spin inversion in these complexes,[13,142] on the yield of O_2^- and OOH radicals and on other important biochemical processes.[160]

References

1. C Schweitzer, R Schmidt *Chem. Rev.* **103** 1685 (2003)
2. V L Ermolaev, E N Bodunov, E B Sveshnikova, T A Shakhverdov *Bezyzluchatel'nyi Perenos Energii Elektronnogo Vozbuzhdeniya* (Non-radiative Transfer of Electronic Excitation Energy) (Leningrad: Nauka, 1977)
3. R Prabhakar, P Siegbahn, B F Minaev, H Agren *J. Phys. Chem. B* **106** 3742 (2002)
4. R S Mulliken *Phys. Rev.* **32** 186 (1928)
5. A White, Ph Handler, E Smith *Principles of Biochemistry* (New York: McGraw-Hill, 1978)
6. D T Sawyer *Oxygen Chemistry* (Oxford: Oxford University Press, 1991)
7. A N Terenin *Fotonika Molekul Krasitelei i Rodstvennykh Organicheskikh Soedinenii* (Photonics of Dye Molecules and Related Organic Compounds) (Leningrad: Nauka, 1967)
8. N N Semenov *O Nekotorykh Problemakh Khimicheskoi Kinetiki i Reaktsionnoi Sposobnosti* (Some Problems of Chemical Kinetics and Reactivity) (Moscow: Academy of Sciences of the USSR, 1958)
9. K-P Huber, G Herzberg *Molecular Spectra and Molecular Structure* (New York: Van Nostrand, 1979)
10. M Kasha, D E Brabham *Singlet Oxygen* (Eds H H Wasserman, R W Murray) (New York: Academic Press, 1979) p. 1
11. J H Van Vleck *Astrophys. J.* **80** 161 (1934)
12. B F Minaev, Doctoral Thesis in Chemical Sciences, Institute of Chemical Physics, Academy of Sciences of the USSR, Moscow, 1983
13. Z M Muldakhmetov, B F Minaev, G A Ketsle *Opticheskie i Magnitnye Svoistva Tripletnogo Sostoyaniya* (Optical and Magnetic Properties of the Triplet State) (Alma-Ata: Nauka, 1983) p. 263
14. A A Krasnovskii Jr *Biofizika* **21** 748 (1976) [a]
15. J Murrell, S Kettle, J Tedder *Valence Theory* (London: Wiley, 1966)
16. R N Zare *Angular Momentum* (New York: Wiley, 1988)
17. P R Ogilby *Acc. Chem. Res.* **32** 512 (1999)
18. D Datta, N Vaidehi, X Xu, W A Goddard *Proc. Natl. Acad. Sci. USA* **99** 2636 (2002)
19. E L Clennan *Acc. Chem. Res.* **34** 875 (2001)
20. R W Redmond, J N Gamlin *Photochem. Photobiol.* **70** 391 (1999)
21. A A Gorman *Adv. Photochem.* **17** 217 (1992)
22. B F Minaev *Izv. Vyssh. Uchebn. Zaved., Fiz.* (9) 115 (1978) [b]
23. B F Minaev *Opt. Spektroskop.* **32** 22 (1972) [c]
24. B F Minaev *Opt. Spektroskop.* **45** 936 (1978) [c]
25. B F Minaev *Int. J. Quant. Chem.* **89** 367 (1980)
26. E V Sveshnikova, B F Minaev *Opt. Spektroskop.* **54** 542 (1983) [c]
27. B F Minaev *Zh. Prikl. Spektroskop.* **42** 766 (1985) [d]
28. B F Minaev *Opt. Spektroskop.* **58** 1238 (1985) [c]
29. B F Minaev *Zh. Strukt. Khim.* **23** 7 (1982) [e]
30. B F Minaev, V A Minaeva *Phys. Chem. Chem. Phys.* **3** 720 (2001)
31. B F Minaev *Phys. Chem. Chem. Phys.* **1** 3403 (1999)
32. B F Minaev, H Agren *Collect. Czech. Chem. Commun.* **60** 339 (1995)
33. B F Minaev, H Agren *Int. J. Quant. Chem.* **57** 519 (1996)
34. B F Minaev *Bull. Pol. Acad. Sci. Chem.* **49** 27 (2001)
35. R Schmidt *Chem. Phys.* **304** 315 (2004)
36. N Dam, T Keszthelyi, L K Andersen, K V Mikkelsen, P Ogilby *J. Phys. Chem. A* **106** 5263 (2002)
37. B F Minaev *RIKEN Rev.* **44** 147 (2002)
38. B F Minaev *Opt. Spektroskop.* **36** 275 (1974) [c]
39. E H Fink, K D Setzer, J Wildt, D A Ramsay, M Vervloet *Int. J. Quant. Chem.* **39** 287 (1991)
40. B F Minaev *Spectrochim. Acta, A* **60** 1027 (2004)

41. O Vahtras, B F Minaev, H Ågren *Chem. Phys. Lett.* **281** 186 (1997)
42. B A Hess, C M Marian, S D Peyerimhoff *Modern Electronic Structure Theory* Pt I (Ed. D R Yarkoney) (Singapore: World Scientist, 1995) p. 152
43. M J Paterson, O Christiansen, F Jensen, P Ogilby *Photochem. Photobiol.* **82** 1136 (2006)
44. U Freichs-Deeken, K Ranguelova, R Kappl *Biochemistry* **43** 14485 (2004)
45. R Prabhakar, P Siegbahn, B F Minaev, H Ågren *J. Phys. Chem. B* **108** 13882 (2004)
46. O Vahtras, O Loboda, B F Minaev, H Ågren *Chem. Phys.* **279** 133 (2002)
47. S R Langhoff *J. Chem. Phys.* **61** 1708 (1974)
48. O Zamani-Khamiri, H F Hameka *J. Chem. Phys.* **55** 2191 (1971)
49. H Lefebvre-Brion, R Field *Perturbation in the Spectra of Diatomic Molecules* (Orlando: Academic Press, 1986)
50. B F Minaev, O Vahtras, H Ågren *Chem. Phys.* **208** 299 (1996)
51. A C Becker, U Schurath, H Dubost, J P Galaup *Chem. Phys.* **125** 321 (1988)
52. G Tuczkowski, U Schurath, M Bodenbinde, H Willner *Chem. Phys.* **215** 379 (1997)
53. T D Poulsen, P R Ogilby, K V Mikkelsen *J. Phys. Chem. A* **102** 8970 (1998)
54. T D Poulsen, P R Ogilby, K V Mikkelsen *J. Phys. Chem. A* **103** 3418 (1999)
55. K M Ervin, W Anusiewicz, P Skurski *J. Phys. Chem. A* **107** 8521 (2003)
56. L K Andersen, P Ogilby *Photochem. Photobiol.* **73** 489 (2001)
57. R Klotz, C M Marian, S D Peyerimhoff, B A Hess, R J Buenker *Chem. Phys.* **89** 223 (1984)
58. P-T Chou, H Frei *Chem. Phys. Lett.* **122** 87 (1985)
59. B F Minaev, Candidate Thesis in Physical and Mathematical Sciences, Tomsk State University, Tomsk, 1973
60. A A Krasnovsky Jr. *Photochem. Photobiol.* **29** 29 (1979)
61. I M Byteva, G P Gurinovich, S P Izbavitelev *Zh. Prikl. Spektroskop.* **23** 285 (1978) [d]
62. K I Salokhiddinov, I M Byteva, G P Gurinovich *Zh. Prikl. Spektroskop.* **34** 92 (1981) [d]
63. A A Krasnovsky Jr *Chem. Phys. Lett.* **81** 443 (1981)
64. M Hild, R Schmidt *J. Phys. Chem. A* **103** 6091 (1999)
65. R Klotz, S D Peyerimhoff *Mol. Phys.* **57** 573 (1986)
66. B F Minaev, L G Telyatnik *Opt. Spektroskop.* **91** 883 (2001) [c]
67. B F Minaev, Z M Muldakhmetov *Opt. Spektroskop.* **56** 48 (1984) [c]
68. A C Becker, U Schurath *Chem. Phys. Lett* **160** 586 (1989)
69. A U Khan, M Kasha *Proc. Natl. Acad. Sci. USA* **76** 6047 (1979)
70. B F Minaev, V S Cherkasov *Opt. Spektroskop.* **45** 264 (1978) [c]
71. B F Minaev, K V Mikkelsen, H Ågren *Chem. Phys. Lett.* **220** 79 (1997)
72. R P Saxon, B Liu *J. Chem. Phys.* **67** 5432 (1977)
73. A P Darmanyan *Chem. Phys. Lett.* **215** 477 (1993)
74. A P Darmanyan *J. Phys. Chem. A* **102** 9833 (1998)
75. K I Salokhiddinov, B M Dzagharov, I M Byteva, G P Gurinovich *Chem. Phys. Lett.* **76** 85 (1980)
76. J R Hurst, J D McDonald, G B Schuster *J. Am. Chem. Soc.* **104** 2065 (1982)
77. P R Ogilby, C S Foote *J. Am. Chem. Soc.* **105** 3423 (1983)
78. P B Merkel, D R Kearns *J. Am. Chem. Soc.* **94** 7244 (1972)
79. B F Minaev *Mol. Eng.* **6** 261 (1996)
80. J N Murrell *Mol. Phys.* **3** 319 (1960)
81. G J Hoijtink *Mol. Phys.* **3** 60 (1960)
82. L K Andersen, P Ogilby *J. Phys. Chem. A* **106** 11064 (2002)
83. L K Andersen, P Ogilby *Rev. Sci. Instrum.* **73** 4313 (2002)
84. H Ågren, O Vahtras, B F Minaev *Adv. Quant. Chem.* **27** 71 (1996)
85. B F Minaev, S Lunell, G I Kobzev *Int. J. Quant. Chem.* **50** 279 (1994)
86. B F Minaev *J. Mol. Struct. (THEOCHEM)* **183** 207 (1989)
87. B F Minaev, H Ågren *J. Chem. Soc., Faraday Trans.* **93** 223 (1997)
88. B F Minaev, S Lunell, G I Kobzev *J. Mol. Struct. (THEOCHEM)* **284** 1 (1993)
89. J F Noxon *Can. J. Phys.* **39** 1110 (1961)
90. C Long, D R Kearns *J. Chem. Phys.* **59** 5729 (1973)
91. B F Minaev *Chem. Phys.* **252** 25 (2000)
92. B R Lewis, S T Gibson, T G Slanger, D L Huestis *J. Chem. Phys.* **110** 11129 (1999)
93. Y Luo, H Ågren, B F Minaev, P Jorgenson *J. Mol. Struct. (THEOCHEM)* **336** 61 (1995)
94. T G Slanger, R A Copeland *Chem. Rev.* **104** 1229 (2004)
95. B F Minaev, L B Yashchuk *Khim. Vys. Energ.* **38** 243 (2004) [f]
96. M C G N van Vroonhoven, G C Groenenboom *J. Chem. Phys.* **117** 5240 (2002)
97. S Langhoff, C Kern *Methods of Electronic Structure Theory* Vol. 4 (Ed. H Schaeffer) (New York: Plenum Press, 1977)
98. B F Minaev, G I Kobzev *Spectrochim. Acta, A* **59** 3387 (2003)
99. B F Minaev *Zh. Fiz. Khim.* **68** 1228 (1994) [g]
100. B F Minaev, E I Fedulova, N M Ivanova, G I Kobzev, Z M Muldakhmetov *Zh. Prikl. Spektroskop.* **67** 453 (2000) [d]
101. A P Losev, I M Byteva, G P Gurinovich *Chem. Phys. Lett.* **143** 127 (1988)
102. S Y Egorov, V F Kamalov, N I Koroteev, A A Krasnovsky Jr, B N Toleutaev *Chem. Phys. Lett.* **163** 421 (1989)
103. B F Minaev, G K Mambeterzina *Fotoprotsessy v Atomnykh i Molekulyarnykh Sistemakh* (Photoprocesses in Atomic and Molecular Systems) (Karaganda: Karaganda State University, 1984) p. 35
104. R D Schurlock, P Ogilby *J. Phys. Chem.* **91** 4599 (1987)
105. A A Krasnovsky Jr, C Schweitzer, H Leismann, C Tanielian, E A Luk'yanets *Quant. Electron.* **30** 445 (2000)
106. R Schmidt, M Bodesheim *J. Phys. Chem.* **99** 15919 (1995)
107. B F Minaev, L B Yashchuk *Biopolim. Kletka* **22** 231 (2006)
108. F Okada, H Kajihara, S Koda *Chem. Phys. Lett.* **192** 357 (1992)
109. B F Minaev, V V Kukueva, H Ågren *J. Chem. Soc., Faraday Trans.* **90** 1479 (1994)
110. V K Mikhalko, G M Zhidomirov, O L Lebedev *Zh. Fiz. Khim.* **58** 1857 (1984) [g]
111. D F Evans *J. Chem. Soc.* 1351 (1957)
112. D L Dexter *J. Chem. Phys.* **21** 836 (1953)
113. B F Minaev *Teor. Eksp. Khim.* **21** 594 (1985) [h]
114. P T Chou, A U Khan *Chem. Phys. Lett.* **103** 281 (1984)
115. B F Minaev *Teor. Eksp. Khim.* **20** 209 (1984) [h]
116. J R Hurst, G B Schuster *J. Am. Chem. Soc.* **105** 5756 (1983)
117. M A J Rodgers *J. Am. Chem. Soc.* **105** 6201 (1983)
118. R Schmidt, H-D Brauer *J. Am. Chem. Soc.* **109** 6976 (1987)
119. E A Ogryzlo, C W Tang *J. Am. Chem. Soc.* **92** 5034 (1970)
120. C S Foot, Y C Chang, R W Denny *J. Am. Chem. Soc.* **92** 5216 (1970)
121. R H Young, D Brewer, R A Keller *J. Am. Chem. Soc.* **95** 375 (1973)
122. R H Young, K Wehrly, R L Martin *J. Am. Chem. Soc.* **93** 5774 (1971)
123. R Boehling, A C Becker, B F Minaev, K Seranski, U Schurath *Chem. Phys.* **142** 445 (1990)
124. B F Minaev, E Jansson, M Lindgren *J. Chem. Phys.* **125** 094306 (2006)
125. T G Slanger, P C Cosby, D L Huestis, D E Osterbrock *J. Geophys. Res.* **105** 20557 (2000)
126. A A Krasnovsky Jr, M E Bashtanov, N N Drozdova *Quant. Electron.* **32** 83 (2002)
127. B F Minaev, L B Yashchuk *Opt. Spektroskop.* **95** 553 (2003) [c]
128. D Weldon, T D Poulsen, K V Mikkelsen, P R Ogilby *Photochem. Photobiol.* **70** 369 (1999)
129. B F Minaev *Zh. Fiz. Khim.* **68** 1432 (1994) [g]
130. C Schweitzer, Z Mehrdad, F Shafii, R Schmidt *Phys. Chem. Chem. Phys.* **3** 3095 (2001)
131. C Schweitzer, Z Mehrdad, A Noll, E-W Grabner, R Schmidt *J. Phys. Chem. A* **107** 2192 (2003)
132. B F Minaev *Khim. Fiz.* **3** 983 (1984) [i]
133. G I Kobzev, Doctoral Thesis in Chemical Sciences, Bashkir State University, Ufa, 2006
134. G I Kobzev, B F Minaev *Zh. Fiz. Khim.* **79** 152 (2005) [g]
135. B F Minaev, V A Tikhomirov *Zh. Fiz. Khim.* **58** 646 (1984) [g]
136. B F Minaev, V A Tikhomirov, Zh K Dausheev *Khim. Fiz.* **3** 615 (1984) [i]
137. B F Minaev, L B Yashchuk *Visn. Odes. Nats. Univ., Ser. Khim.* **9** 52 (2004)
138. B F Minaev *Zh. Fiz. Khim.* **66** 2992 (1992) [i]

139. I V Savitskii *Biologicheskaya Khimiya* (Biological Chemistry) (Kiev: Vishcha Shkola, 1982)
140. M Engstrem, B F Minaev, O Vahtras, H Ågren *Chem. Phys.* **237** 149 (1998)
141. G Herzberg *Science* **177** 123 (1972)
142. Yu A Serebrennikov, B F Minaev, B Abdrakhmanov *Khim. Fiz.* **5** 878 (1986) [i]
143. T C Brunold, E I Solomon *J. Am. Chem. Soc.* **121** 8277 (1999)
144. T C Brunold, E I Solomon *J. Am. Chem. Soc.* **121** 8288 (1999)
145. B F Minaev *Ukr. Biokhim. Zh.* **74** 11 (2002) [j]
146. A Bassan, M R Blomberg, P Siegbahn *Eur. J. Chem. A* **9** 106 (2003)
147. J N Harvey *Faraday Disc.* **127** 165 (2004)
148. B F Minaev *Visn. Cherkas. Inzh.-Tekhnol. In-tu* (3) 6 (2001)
149. R Prabhakar, P Siegbahn, B Minaev *Biochim. Biophys. Acta Proteins Proteomics* **1647** 173 (2003)
150. B F Minaev, V A Minaeva, V N Leshchenko *Biopolim. Kletka* **20** 1 (2004)
151. V A Belyakov, R F Vasil'ev, N M Ivanova, B F Minaev *Izv. Akad. Nauk SSSR, Ser. Fiz.* **51** 540 (1987) [k]
152. J P Klinman *J. Biol. Inorg. Chem.* **6** 1 (2001)
153. J P Roth, J P Klinman *Proc. Natl. Acad. Sci. USA* **100** 62 (2003)
154. B F Minaev *Opt. Spektroskop.* **80** 407 (1996) [c]
155. M F Gulyi, V I Bilai, N M Pidoplichko, R G Degtyar', E A Nikol'skaya *Ferment Glyukozooksidaza i Ego Primenenie* (The Glucose Oxidase Enzyme and Its Applications) (Kiev: Naukova Dumka, 1964)
156. P E M Siegbahn *Inorg. Chem.* **38** 2880 (1999)
157. P E M Siegbahn *J. Comput. Chem.* **22** 1634 (2001)
158. P E M Siegbahn, M R A Blomberg *Chem. Rev.* **100** 421 (2000)
159. S Shaik, M Filatov, D Schroder, H Schwarz *Chem. – Eur. J.* **4** 193 (1998)
160. L A Buchachenko, R Z Sagdeev, K M Salikhov *Magnitnye i Spinovye Effekty v Khimicheskikh Reaktsiyakh* (Magnetic and Spin Effects in Chemical Reactions) (Novosibirsk: Nauka, 1978)
161. Yu A Serebrennikov, B F Minaev, B Abdrakhmanov *Khim. Fiz.* **6** 799 (1987) [i]
162. L A Buchachenko *Usp. Khim.* **59** 529 (1990) [*Russ. Chem. Rev.* **59** 307 (1990)]
163. S V Vonsovskii *Magnetizm* (Magnetism) (Moscow: Nauka, 1971)
164. R White *Quantum Theory of Magnetism* (New York: McGraw-Hill, 1970)

[a] — *Biophysics (Engl. Transl.)*
[b] — *Russ. Phys. J. (Engl. Transl.)*
[c] — *Opt. Spectroscop. (Engl. Transl.)*
[d] — *J. Appl. Spectroscop. (Engl. Transl.)*
[e] — *J. Struct. Chem. (Engl. Transl.)*
[f] — *High Energ. Chem. (Engl. Transl.)*
[g] — *Russ. J. Phys. Chem. (Engl. Transl.)*
[h] — *Theor. Exp. Chem. (Engl. Transl.)*
[i] — *Chem. Phys. Rep. (Engl. Transl.)*
[j] — *Ukr. Biochem. J. (Engl. Transl.)*
[k] — *Bull. Russ. Acad. Sci., Phys. (Engl. Transl.)*